

Linear-Size Ancilla Systems for Logical Measurements in QLDPC Codes

Andrew Cross¹, Zhiyang He (Sunny)², Patrick Rall³, and Theodore Yoder¹

¹IBM Quantum, IBM T.J. Watson Research Center

²Massachusetts Institute of Technology

³IBM Quantum, IBM Research Cambridge

July 29, 2024

Abstract

We show how to perform all logical Clifford gates on the $[[144,12,12]]$ bivariate bicycle code, also known as the gross code. The scheme adds about 100 ancilla qubits into the connectivity graph, and one of the twelve logical qubits is sacrificed for gate synthesis. Logical measurements are combined with the automorphism gates studied by Bravyi et al. (Nature 627, 778-782) to implement 288 Pauli product measurements. We demonstrate the practicality of our scheme through circuit-level noise simulations, leveraging a novel modular decoder that combines BPOSD with matching.

The main technical contribution is a lower overhead logical measurement scheme based on gauge-fixing the construction by Cohen et al. (Sci. Adv. 8, eabn1717). Our techniques apply to general CSS codes and leverage expansion properties of the Tanner graph to give rigorous guarantees on qubit count, code distance, fault distance, and decoding distance of the modular decoder. In particular, we require $O(d/\beta)$ additional qubits where β is the boundary Cheeger constant of the subgraph supporting the logical operator being measured. By introducing $O(d)$ additional bridge qubits, we are also able to measure products of logical Pauli operators and logical Y operators.

Contents

1	Introduction	2
2	Preliminaries	4
2.1	Tanner graph notation	5
2.2	The CKBB ancilla system	5
3	Gauged Ancilla Systems	6
3.1	Gauged X Ancilla Systems	7
3.2	X Measurement Protocol	8
3.3	Code Distance and Fault Distance	10
3.4	Modular Decoder Achieving Measurement Fault-Distance	15
3.5	Joint X Measurement	17
3.6	Gauged Y Ancilla System	21
4	Case Study: Gross Code	24
4.1	Mono-layer ancilla system	26
4.2	Numerical simulations	27
4.3	Implementing logical Clifford gates	29
5	Future Work	31

A Appendices	32
A.1 Proofs for the X Ancilla System	32
A.2 Proofs for the Y Ancilla System	34

1 Introduction

Reliable quantum computing at scale requires encoding quantum information into error-correcting codes and acting on that information without spreading errors too quickly [ABO08, Kit97, KLZ98, AGP05, Got09]. This necessitates a fault-tolerant architecture that both stores quantum information and also computes with it [CTV17]. The surface code provides the foundation for one of the leading fault-tolerant quantum computing architectures [BK98, DKLP02, FMMC12, Lit19]. It has a high accuracy threshold, allowing it to tolerate realistic noise rates, and its low-weight, geometrically local check operators can be measured on hardware that implements a two-dimensional lattice [KLR⁺22, AI23, SYK⁺23].

The technique of lattice surgery is an essential element of the surface code architecture that enables computation at realistic noise rates within the same local connectivity of the code itself [HFDM12]. Lattice surgery provides a way to measure products of logical Pauli operators by measuring many low-weight geometrically local checks. Not all of these checks belong to the code when they are measured, so the code changes dynamically by a process called gauge fixing [VLC⁺19]. Sequences of lattice surgery operations implement the subset of logical gates called Clifford gates. The surface code architecture is completed by incorporating magic state injection and distillation to construct a universal set of gates [BK05, Li15, Lit19, CC22].

However, the surface code architecture comes with significant overhead. Resource estimates for scaled applications indicate that surface code architectures may require many millions of qubits [GE21, BMT⁺22]. One of the reasons for this daunting space overhead is that codes that are constrained to have local checks in two dimensions, such as the surface code, have parameters that are governed by the Bravyi-Poulin-Terhal bound [BPT10]. This bound limits how efficiently codes with geometrically local checks encode quantum information. An implication is that, because the surface code is the exemplar of all such geometrically local codes, it is difficult to find better codes under these constraints.

One way forward is to relax the requirement of geometric locality, while retaining the need for qubits and checks to connect to only a few neighbors. Such high-rate low-density parity check (LDPC) codes can have much better parameters, both in terms of their encoding rate and their ability to correct errors [TZ14, PK21, BE21b, BE21a, PK22, LZ22]. Using these codes, fault-tolerant quantum computing becomes possible in principle with only constant space overhead in the asymptotic limit [Got14, FGL20].

Recently, protocols for quantum memories based on LDPC codes have been discovered [BVC⁺17, NFB17, HB23, BCG⁺24, XAP⁺24]. Efficient memories could be used in concert with the surface code to reduce space overhead. In some instances, these memory protocols simultaneously have high thresholds and low overheads at practical code block sizes, making them attractive candidates for near-term demonstrations [BCG⁺24]. A growing body of research aims to find improved codes [SHR24, VXHB24], decoders [GCR24, WB24], and implementations for these quantum memories [VYL⁺23, PGP⁺24, BDS⁺24].

Beyond storing information in high-rate quantum LDPC codes, computing directly on that information is an active area of research. There is the need for fast, parallel, and space-efficient gates, and also the challenge that logical qubits are encoded together in the same block, making them difficult to address individually. For stabilizer codes, there is a general solution that teleports qubits or gates and measures logical observables using specially prepared ancilla states [Got97, GC99, SI05, Kni05]. However, these large Steane- or Knill-type ancilla states are expensive to prepare, so new methods have been developed that are specific to LDPC codes [BVC⁺17, LB18, JO19, KP21, CKBB22, HJOY23, ZSP⁺23]. A subset of these approaches generalize the idea of lattice surgery to codes other than the surface code [BVC⁺17, LB18, KP21, CKBB22]. The methods can be complemented by symmetry-based gates, such as transversal and fold-transversal gates [QWV23, BB24, ES24].

In this paper, we consider the problem of computing with LDPC codes using generalized lattice surgery. Our high level goal is to efficiently measure a set of logical Pauli operators of one or more LDPC code blocks.

There are two simple, well-known ways to measure a weight d logical operator: individually measure each qubit in the support of the logical operator and infer the logical qubit state, or entangle a single ancilla qubit to the operator using d CNOT gates and measure the ancilla. It is easy to see that the first method can be highly disruptive to the remaining logical information, while the second method requires qubit degree $d + 1$ and is not fault-tolerant, since an error on the ancilla can propagate to many other qubits. The problem of designing logical measurement schemes, therefore, is to obtain the measurement result fault-tolerantly while maintaining sparse connectivity and reasonable space overhead. We build on the merged codes and ancilla systems introduced by Cohen, Kim, Bartlett, and Brown [CKBB22], which are an application of stabilizer weight reduction techniques [Has21, SGI⁺24].

We measure the quality of a logical measurement scheme in terms of four metrics: space-time overhead, parallelism, connectivity, and fault-tolerance. Let us now describe these metrics.

1. Space-time overhead: A scheme requires a system of ancilla qubits to implement a set of measurements. The total number of qubits in this system is an important metric. A circuit acting on the original code and the ancilla system enacts the measurement. The depth of this measurement circuit is another key metric.
2. Parallelism: Commuting logical operators can be measured simultaneously. A scheme allows some set of measurements to occur in parallel.
3. Connectivity: Extending the code with an ancilla system means adding more connections between qubits. Connections are needed between pairs of qubits that interact. In this paper, the connections correspond to edges in the Tanner graph of a quantum code. We measure this cost in terms of qubit degree, which is the maximum number of neighboring qubits connected to a single physical qubit.
4. Fault-tolerance: There are several ways to measure the fault-tolerance of a scheme. In this paper, we study the following measures.
 - (a) Code distance: During the measurement procedure, the base LDPC code changes into a merged code. The logical information is protected by a subsystem code with all the logical qubits from the original code (except the one being measured), and some gauge qubits which carry no logical information. Ideally, this subsystem code should have distance d , so that the unmeasured logical information remains well-protected.
 - (b) Fault distance: Besides the subsystem code distance, we also consider the phenomenological fault distance of logical measurement schemes, which is the minimum number of measurement or qubit errors needed to produce a logical error or an incorrect logical measurement outcome without triggering any detectors. A logical measurement scheme should have fault distance d . We further distinguish between the logical fault distance and the measurement fault distance in our analysis.
 - (c) Circuit distance: The procedure is implemented by a noisy quantum circuit whose gates and other circuit locations can fail. The circuit distance is the minimum number of faults needed to produce a logical error or incorrect logical measurement outcome without triggering any detectors. Ideally, a logical measurement circuit should have circuit distance d .

The major goals of this paper are to significantly reduce the space overhead of the CKBB scheme and apply our results to a practically-motivated case study. Our scheme, which we name the *gauged ancilla system*, improves upon the CKBB scheme by gauge-fixing low-weight operators that may otherwise harm the distance of the merged code. We further improve the scheme by introducing *bridge* qubits to preserve distance during joint measurements. As we will show, these techniques, together with careful choice of what logical operators to measure, result in substantial improvement in space overhead.

Our central result is the proposed gauged ancilla system, which we put forward as a practical approach to fault-tolerantly measuring logical information in LDPC codes. We show that the number of layers in the ancilla system can be greatly reduced in general if the Tanner graph induced by the logical operator is suitably expanding; see Table 1. We further present proposals for gauged Y and joint measurement ancilla

systems, as well as a modular decoding technique to reduce the decoding complexity during the logical measurement protocol. We systematically analyze the fault-tolerance properties of our proposals.

	Ref [CKBB22]	Theorem 6 in this paper
Ancilla system size	$O(d^2)$	$O(d/\beta)$
Bound on number of layers L	$L \geq 2d - 1$	$\lceil L/2 \rceil \geq 1/\beta$

Table 1: Parameters of merged codes with code distance d . The parameter β is the boundary Cheeger constant of the Tanner graph induced by the logical observable.

Bringing our central results together, we present an in-depth study of a logical measurement scheme for the $[[144, 12, 12]]$ gross code, a 6-limited bivariate bicycle code [BCG⁺24]. In particular, we demonstrate that a mono-layer, degree-8 ancilla system with 103 additional qubits suffices to measure eight distinct logical Pauli operators, which significantly improves on the state of the art as summarized in Table 2. In this connectivity graph exactly two qubits have degree 8, and the remaining ones have degree 7 or less. We numerically study the logical error rates of \bar{X} and \bar{Z} logical measurements under circuit-level noise and find they are within a factor of 10x and 5x larger than that of the base code, respectively. We find that seven repetitions of the merged code syndrome measurement optimizes the logical and measurement error rates at a physical error rate of 0.001. We see that modular decoding gives comparable logical error rates to BPOSD but significantly improves decoding time. Finally, we combine permutation automorphisms with logical measurements to implement a set of 288 native Pauli measurements on the 12 logical qubits. This yields a further set of 95 Pauli rotations $\{\exp(i\frac{\pi}{4}P)\}$ that generate the eleven-qubit Clifford group within the gross code block. Furthermore the twelve logical qubits can be individually measured.

	Ref [BCG ⁺ 24]	Ref [Cow24]	This work
Measurement set	$X(f, 0),$ $Z(h^\top, g^\top)$	$X(f, 0),$ $Z(h^\top, g^\top)$	$\bar{X} := X(p, q), \bar{Z} := Z(r, s),$ $\bar{X}' := X(ws^\top, wr^\top), \bar{Z}' := Z(wq^\top, wp^\top),$ $\bar{Y} := i\bar{X}\bar{Z}, \bar{Y}' := i\bar{X}'\bar{Z}',$ $\bar{X}\bar{X}', \bar{Z}\bar{Z}'$
Ancilla system size	1380	180	103
Number of layers	23	5	1
Maximum qubit degree	7	7	8

Table 2: Parameters of logical measurement schemes for the $[[144, 12, 12]]$ gross code. Each scheme allows one measurement from the measurement set to be performed at a time. The Pauli operators in the measurement set are presented using the notation of [BCG⁺24]. The number of layers is the maximum over all merged codes in the scheme. We note that [Cow24] presents different versions with varying amounts of parallelism and size; we choose a version that is most similar to [BCG⁺24].

The paper is organized as follows. Section 2 establishes notation and reviews the CKBB measurement scheme. Section 3 presents our low-overhead gauged ancilla systems for CSS codes, describes our modular decoding technique, and establishes the fault-tolerance properties of the systems and measurement protocols. In Section 4, we apply these techniques to construct an ancilla system for the $[[144, 12, 12]]$ gross code, numerically investigate its performance in the circuit model, and synthesize logical Clifford gates on the code block.

2 Preliminaries

We begin by establishing some notation. We then apply this notation to review the logical measurement scheme presented by [CKBB22].

2.1 Tanner graph notation

Consider a CSS code \mathcal{G} with check matrices $H^X \in \mathbb{F}_2^{m_x \times n}$, $H^Z \in \mathbb{F}_2^{m_z \times n}$ and minimum distance d . Let \mathcal{V} denote the set of qubits, with $|\mathcal{V}| = n$, \mathcal{C}^Z denote the set of Z -checks with $|\mathcal{C}^Z| = m_z$, and \mathcal{C}^X denote the set of X -checks with $|\mathcal{C}^X| = m_x$. The *Tanner graph* is a tripartite graph with vertex sets $\mathcal{C}^X, \mathcal{V}, \mathcal{C}^Z$ such that each vertex in \mathcal{C}^X and \mathcal{C}^Z is connected to the qubits they act on in \mathcal{V} .

We describe quantum codes with or without ancilla systems by drawing their Tanner graphs. Instead of drawing the Tanner graphs in their entirety, we combine nodes into several sets of either check nodes or qubit nodes. These sets should be chosen so that we can easily describe the connections between each pair of qubit and check sets via an incidence matrix. To be more specific, if there is a set of qubits V and a set of checks C , the edge between them will be labeled by a matrix $F \in \mathbb{F}_2^{|C| \times |V|}$ where $F_{ij} = 1$ if and only if check i from C is connected to qubit j from V . If these checks are Z checks, then we use \rightarrow_Z to summarize the above situation as $F : C \rightarrow_Z V$. For example the code \mathcal{G} above has connections $H^X : \mathcal{C}^X \rightarrow_X \mathcal{V}$ and $H^Z : \mathcal{C}^Z \rightarrow_Z \mathcal{V}$. Since our graphs are sparse, many pairs of qubit and check sets will not be connected (or, formally, connected by the 0 matrix), in which case we leave out that edge.

This way of drawing the Tanner graph is essentially a description of the code as a chain complex. We can therefore think of sets of checks C and sets of qubits V as vector spaces over \mathbb{F}_2 with F the boundary map between them. A subset $c \subset C$ can be seen as a row vector in $\mathbb{F}_2^{|C|}$. Then, if $F : C \rightarrow_Z V$, the qubits in V that correspond to the product of the subset of checks c in C are $v = cF \in \mathbb{F}_2^{|V|}$.

In our figures, an edge denoting the connection $F : C \rightarrow_Z V$ is labeled by the matrix F as well as the Pauli matrix Z , or X, Y for $\rightarrow_X, \rightarrow_Y$ respectively, to indicate how the checks act on connected qubits. When all edges from a set of check nodes are labeled the same, we simply label the set of check nodes with X, Y , or Z . Checks are always rows and qubits are always columns, although vectors are always row vectors.

To specify the type of Pauli explicitly, we adopt the notation $Z(v \in V)$ (or $X(\cdot)$ or $Y(\cdot)$), to indicate Pauli Z s acting on exactly the qubits indicated by v . If it is clear from context that v is a member of V , then we can shorten this to $Z(v)$. If we want Z to act on all qubits in V , we write simply $Z(V)$.

Similarly, we indicate a product of checks by $\mathcal{H}(c \in C) = \mathcal{H}(c)$ and the product of all checks in C by $\mathcal{H}(C)$. We also use $\mathcal{H}_Z(\cdot)$ or $\mathcal{H}_X(\cdot)$ if the checks are entirely Z - or X -type, respectively. This is meant to indicate the Pauli operator obtained by multiplying together the checks indicated by vector c . For example, if $F : C \rightarrow_Z V$, then $\mathcal{H}_Z(c \in C) = Z(cF \in V)$.

Finally, if two Paulis P_1, P_2 differ only by an element of a Pauli group \mathcal{S} , i.e. $P_1 = sP_2$ for $s \in \mathcal{S}$, we write $P_1 \equiv_{\mathcal{S}} P_2$.

2.2 The CKBB ancilla system

Consider any CSS code \mathcal{G} . In general, we say a logical X operator \bar{X}_M is irreducible if there are no other logical X operators whose support is a subset of that of \bar{X} . We focus on logical X operators here, but an ancilla system for Z operators can be obtained by swapping X and Z in the construction. In the measurement scheme introduced by [CKBB22], for any logical operator \bar{X}_M that is irreducible, they create an extended Tanner graph with \bar{X}_M in the stabilizer.

Key to their construction and ours is the subgraph consisting of \bar{X}_M and its neighborhood of Z checks. For an X -logical operator \bar{X}_M supported on a set of qubits $V_0 \subset \mathcal{V}$, let $C_0 \subset \mathcal{C}^Z$ be the set of Z -checks that has neighbors in V_0 . The induced Tanner graph of \bar{X}_M is the restriction of the Tanner graph to the vertices V_0 and C_0 . Formally, since the induced Tanner graph only features Z checks, we can define a matrix $F : C_0 \rightarrow_Z V_0$ whose rows are the supports of the Z checks. If $J_{V_0} : \mathcal{V} \rightarrow V_0$ and $J_{C_0} : \mathcal{C}^Z \rightarrow C_0$ are projection isometries, then $F := J_{C_0}^\top H^Z J_{V_0}$.

A pair of V_i, C_i , connected as in the Tanner graph constitute one ‘layer’ of the construction. Having identified C_0, V_0 within the original code \mathcal{G} ’s vertices $\mathcal{C}^Z, \mathcal{V}$, we append $2d - 1$ more such layers. We assign

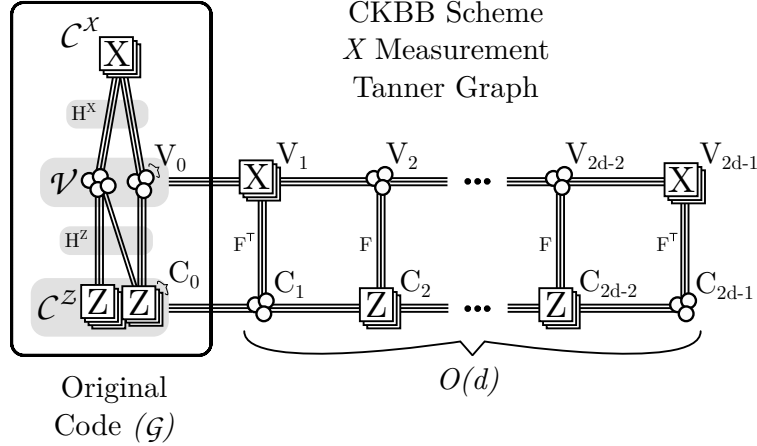


Figure 1: Diagram of the CKBB scheme for measuring a logical X operator. The original code’s Tanner graph is a subgraph of this graph supported on $\mathcal{V}, \mathcal{C}^X$, and \mathcal{C}^Z .

these vertices alternating roles, as follows.

$$V_i \text{ for } \begin{cases} \text{odd } i \rightarrow X \text{ check} \\ \text{even } i \rightarrow \text{physical qubit} \end{cases} \quad (1)$$

$$C_i \text{ for } \begin{cases} \text{odd } i \rightarrow \text{physical qubit} \\ \text{even } i \rightarrow Z \text{ check} \end{cases} \quad (2)$$

Layers are connected identically via $F : C_i \rightarrow_Z V_i$ for even i , and $F^\top : V_i \rightarrow_X C_i$ for odd i . Furthermore, adjacent layers are connected by the identity: $I : C_0 \rightarrow_Z C_1$, $I : V_1 \rightarrow_X C_0$, $I : V_1 \rightarrow_X C_2$, $I : C_2 \rightarrow_Z C_1$, etc. This construction is visualized in Figure 1.

In the resulting code the operator \bar{X}_M is a product of stabilizers, namely all the appended X -checks $V_1, V_3, \dots, V_{2d-1}$. Therefore a code-switching scheme from \mathcal{G} to the larger code can be used for a fault-tolerant logical measurement of \bar{X}_M . If any other logical operators were contained in the support of \bar{X}_M , then these would be measured as well. Therefore it is key that \bar{X}_M is irreducible.

The number of ancilla qubits needed is $(2d - 1)(|V_0| + |C_0|) > 2d^2$, which is a daunting space overhead. For codes where the distance d scales as \sqrt{n} , this number of ancilla qubits may be more than the number of qubits used in the code itself. One of the primary goals of this paper is to reduce this space overhead by using fewer layers. The time overhead is d rounds of error correction which is standard albeit on a bigger code. We observe that if \mathcal{G} has maximum degree D , then the CKBB ancilla system has maximum degree $D + 1$.

The CKBB ancilla system is a subsystem code with all the logical qubits from the original code \mathcal{G} except the one being measured, and some gauge qubits which carry no logical information. It was proven in [CKBB22] that the CKBB ancilla system has code distance d . The fault distance or circuit distance of such a measurement protocol is not known.

3 Gauged Ancilla Systems

In this section we present our main result: a family of lower-overhead ancilla systems that measure logical operators in CSS codes. In sections 3.1 and 3.2 we detail the gauged X ancilla system \mathcal{G}_X , which is similar to the CKBB X ancilla described above but introduces additional gauge checks. In section 3.3 we prove Theorem 6, which relates the distance of the merged quantum code to the ancilla system size and the Cheeger constant of its induced Tanner graph. We introduce a modular decoding architecture in section 3.4.

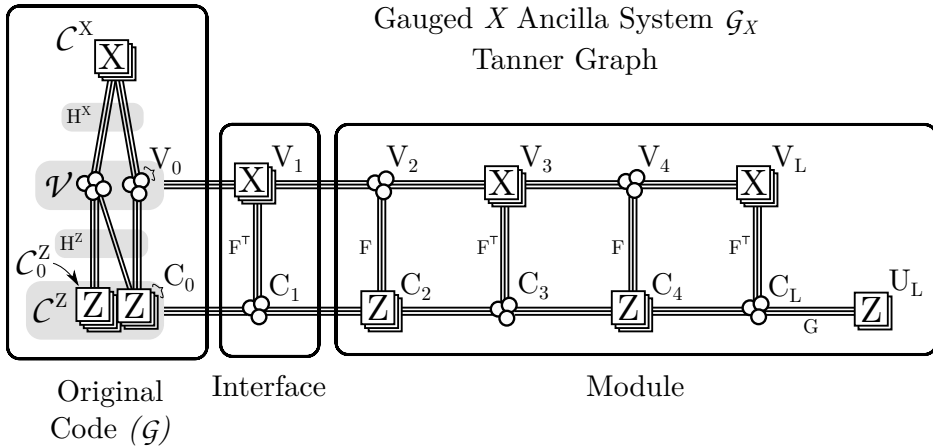


Figure 2: Diagram of the gauged X ancilla system \mathcal{G}_X with $L = 5$. The original code \mathcal{G} 's Tanner graph is a subgraph of this graph supported on $\mathcal{V}, \mathcal{C}^X$, and \mathcal{C}^Z . The first layer (V_1, C_1) is called the interface, and the remaining layers and the gauge checks U_L are called the module.

In sections 3.5 and 3.6 we generalize the construction to multi-qubit measurements \mathcal{G}_{XX} (including between separate codeblocks) and Y measurements \mathcal{G}_Y , which require an additional bridge construction.

3.1 Gauged X Ancilla Systems

We follow the notation used to describe the CKBB scheme in Section 2.2, since the initial part of the construction is the same. Recall that we are measuring an X -logical operator \bar{X}_M with support $V_0 \subset \mathcal{V}$ and adjacent Z -checks $C_0 \subset \mathcal{C}^Z$. As before, we assume there are no other X operators supported on a subset of V_0 . We again consider the induced Tanner graph of \bar{X}_M : let $J_{V_0} : \mathcal{V} \rightarrow V_0$ and $J_{C_0} : \mathcal{C}^Z \rightarrow C_0$ be projection isometries into the corresponding sets, and let F be the submatrix of H^Z defined by $F := J_{C_0}^\top H^Z J_{V_0}$. Then $F : C_0 \rightarrow_Z V_0$ is the adjacency matrix of the induced Tanner graph.

Now we introduce L additional layers $(C_1, V_1), (C_2, V_2), \dots, (C_L, V_L)$ with vertex roles as in Eq. (1) and the connectivity as in the CKBB system with $F : C_i \rightarrow_Z V_i$ for even i , $F^\top : V_i \rightarrow_X C_i$ for odd i and I for connections between layers. So far, if we take $L = 2d - 1$, we have just constructed the CKBB system again.

The CKBB X measurement scheme is a subsystem code with gauge degrees of freedom. These gauge degrees of freedom complicate the analysis in [CKBB22] and are only dealt with in general by using at least $2d - 1$ layers. In our work we simply promote these gauge degrees of freedom to stabilizers, resulting in a non-subsystem stabilizer code \mathcal{G}_X .

The Z gauge operators of the CKBB scheme correspond to the nullspace of F , that is, $\text{null}(F) = \{c \text{ s.t. } cF = 0\}$. This is because the rows of $F^\top : V_i \rightarrow_X C_i$ for odd i denote X checks within the layer (C_i, V_i) , and vectors orthogonal to these rows commute with these X checks. Any particular gauge operator $Z(c)$ has equivalent realizations on any C_j for any odd j , since we can multiply by Z checks in the layers C_i with i even. That is, $Z(c \in C_j)\mathcal{H}_Z(c \in C_{j+1}) = Z(cF \in V_{j+1})Z(c \in C_{j+2}) = Z(c \in C_{j+2})$.

To find a set of additional Z checks that remove these gauge qubits, we find a matrix G whose rows span $\text{null}(F)$, that is, $GF = 0$. Minimizing row and column weight of G minimizes the degree of the Tanner graph. Then we introduce a new set of Z checks U_L and connect $G : U_L \rightarrow_Z C_L$. This completes the construction of \mathcal{G}_X . A sketch of \mathcal{G}_X is shown in Figure 2.

The resulting code has the following properties.

Theorem 1. *Say \mathcal{G} is any CSS code and \bar{X}_M is a X -logical Pauli operator with no smaller X -logical operators in its support. Let \mathcal{G}_X be the code defined above. Then \bar{X}_M is a stabilizer of \mathcal{G}_X , and \mathcal{G}_X has exactly one fewer logical qubit than \mathcal{G} .*

We defer the proof of this theorem to Appendix A.1.

Remark 2. Sometimes the gauge checks in G are already products of other Z stabilizers of \mathcal{G}_X and hence do not need to be added as explicit checks in U_L . This happens for the gross code as we will see in Section 4 and for hypergraph product codes.

3.2 X Measurement Protocol

We now describe the measurement protocol that allows us to extract the measurement result of \bar{X}_M while leaving the remaining logical information undamaged. This is achieved through construction of a decoding hypergraph \mathcal{D} , which is a collection of detectors. We measure the checks of either \mathcal{G} or \mathcal{G}_X for several rounds. Then, a detector is the parity of a subset of these check measurement outcomes, understood as a hyperedge within \mathcal{D} . In this section we consider the noise-free case. Our objective is to demonstrate that, although the check measurement outcomes are sometimes non-deterministic, the detector parities are always zero. We assess the fault-tolerance properties of \mathcal{D} in the next section.

\mathcal{D} splits into steps $\mathcal{D}_0, \dots, \mathcal{D}_R$, corresponding to R measurements of the checks of \mathcal{G}_X . The first and final steps \mathcal{D}_0 and \mathcal{D}_d handle the code deformation between \mathcal{G} and \mathcal{G}_X .

As shown in Figure 2, we call the first layer of \mathcal{G}_X (V_1, C_1) the *interface*, and the remaining layers are the *module*. There is no module when $L = 1$, so the gauge checks U_1 are considered part of the interface. The stabilizers $Z(C_0)$ and $Z(C_2)$ have support on the interface qubits C_1 . Let \tilde{C}_0 and \tilde{C}_2 be modified versions of these checks that are missing support on C_1 . This is useful since \mathcal{G} has no support on the interface, and hence has the Z -stabilizers $Z(\tilde{C}_0)$.

\mathcal{D} is constructed as follows. A small example is shown in Figure 3. In the construction, a check is called *unreliable* if, even in the noise-free case, the outcome of the check is random since it doesn't commute with the stabilizer of the current state. A *reliable* check is deterministic in the noise-free case, but not necessarily $+1$.

1. To initialize:
 - (a) Initialize the interface qubits, namely qubits in C_1 , to $|0\rangle$.
 - (b) If there is a module ($L > 1$), initialize a stabilizer state on the module qubits C_2, V_3, \dots, V_L . It has the stabilizers $Z(\tilde{C}_2), Z(C_i)$ for even $i \geq 4$, $Z(U_L)$, and the $X(V_i)$ for odd $i \geq 3$. We refer to these checks as the *module stabilizer*.
 - (c) Measure the module stabilizers. Additionally, either measure the stabilizers of \mathcal{G} , or consider the measurement outcomes from a prior round. If there is no module ($L = 1$), then we can still compute gauge checks $Z(U_1)$ by measuring the interface qubits in the Z basis and computing the appropriate parities.
2. (Fusion step) Measure the stabilizers of \mathcal{G}_X . Of these, the $X(V_1)$ checks are unreliable, but everything else is reliable. Let \mathcal{D}_0 contain parities between pairs of reliable checks from step 1 and step 2 only. This involves taking parities between step 1's $Z(\tilde{C}_0)$ and step 2's $Z(C_0)$, as well as step 1's $Z(\tilde{C}_2)$ and step 2's $Z(C_2)$. The module stabilizers except $Z(\tilde{C}_2)$ are identical in step 1 and step 2 so these parities are zero. From round 1 to 2, checks $Z(\tilde{C}_0)$ and $Z(\tilde{C}_2)$ have gained support on the interface C_1 and become $Z(C_0)$ and $Z(C_2)$. But since the interface qubits are in the $|0\rangle$ state, the measurement outcome is unaffected, so these parities should be zero as well. Output the parity of the $X(V_1)$ checks as the measurement result, since their product $\mathcal{H}_X(V_1)$ is \bar{X}_M in the noiseless case. This value should be subject to decoder corrections.
3. Measure the stabilizers of \mathcal{G}_X $R - 1 \geq 0$ more times. Let the detectors \mathcal{D}_i for $0 < i < R$ be the parities between successive measurements. Since these are all the same checks, the parities should all vanish.
4. (Split step) Measure the stabilizers of \mathcal{G} . Measure the interface qubits C_1 in the Z basis. Measure the module stabilizers.

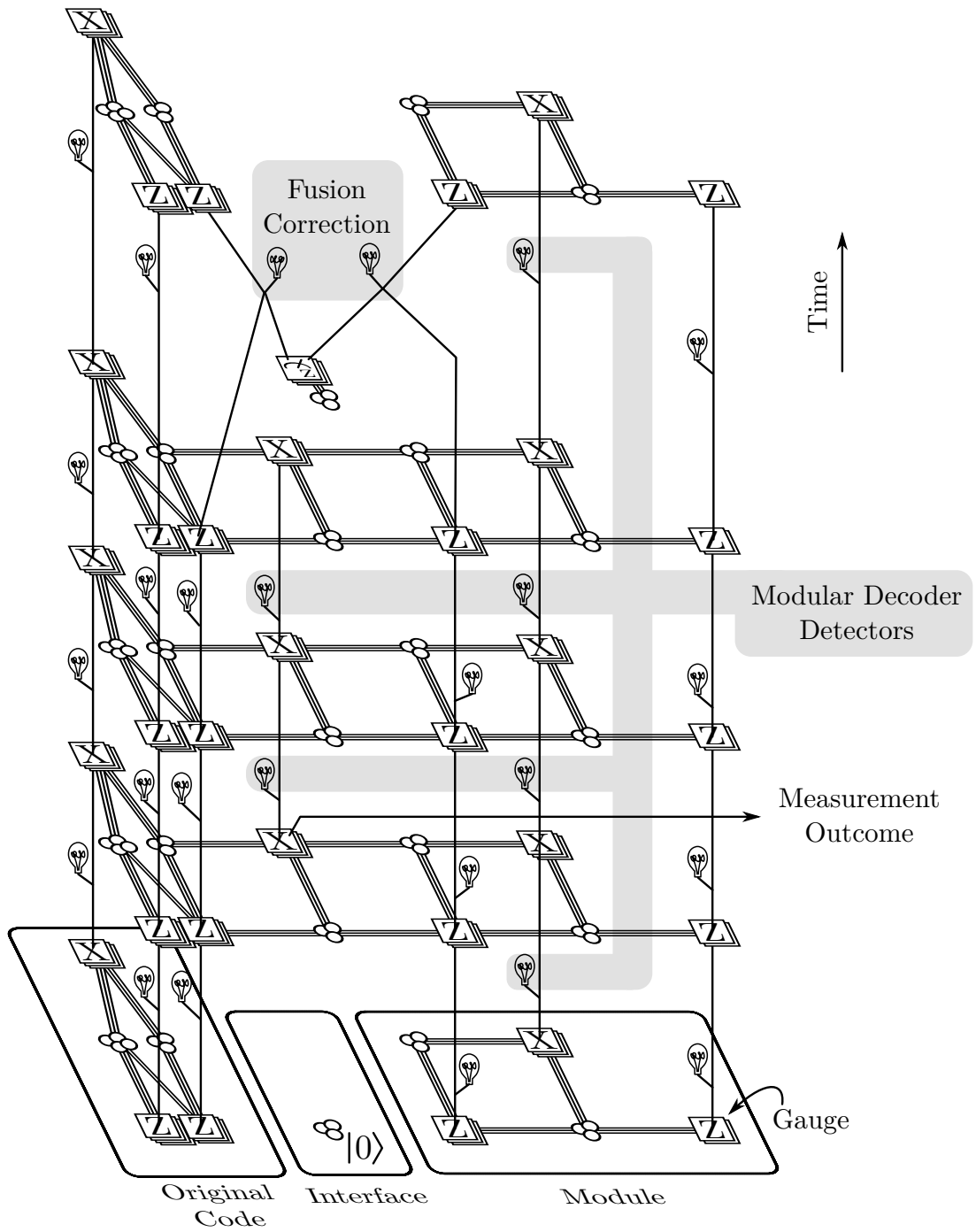


Figure 3: Space-time diagram and matching graph of a measurement protocol using an X ancilla system. Detectors are denoted by lines connecting different checks and a lightbulb symbol. The errors identified by certain detectors can be decoded separately using a modular decoding approach - see section 3.4.

Checks $Z(\tilde{C}_0)$, $Z(\tilde{C}_2)$, and the interface qubit Z -measurements C_1 are all unreliable. However, we can still compute what the outcome of the reliable checks $Z(C_0)$ and $Z(C_2)$ would have been by considering the appropriate parities of $Z(\tilde{C}_0)$, $Z(\tilde{C}_2)$ with the Z -measurements of C_1 . The parities of these values with the measurements of $Z(C_0)$ and $Z(C_2)$ of the prior step feature in \mathcal{D}_R . These are shown as the *fusion correction* in Figure 3.

As in step 1, if there is no module then gauge checks $Z(U_1)$ can still be computed by considering the appropriate parities of the Z measurements of C_1 . \mathcal{D}_R also features detectors comparing these parities to the $Z(U_1)$ measurement from the prior round.

The initialization of the module can be done independently and in advance. The module when viewed as a code itself has no logical qubits — it is a single stabilizer state. Therefore, the module is reusable in future rounds of logical measurements, if we keep it error-free. In other words, the module can be viewed as a resource state that facilitates fault-tolerant logical measurements. A similar module system appeared for a different purpose in [XAP⁺24].

Although we let $R \geq 1$, the number of times the stabilizers of the merged code \mathcal{G}_X are measured, be arbitrary in this description, we will conclude below in Theorem 11 that $R \geq d$ is sufficient for the fault-tolerance of the protocol. In practice, we may want to balance logical error rates and the error rate of the logical measurement, and this may mean $R < d$ offers better performance. We probe this trade-off in our case study in Section 4.

3.3 Code Distance and Fault Distance

We demonstrate that, if the original code \mathcal{G} has distance d , then there exists a choice of layers L such that \mathcal{G}_X also has distance d . With L chosen as such, we then demonstrate that the fault distance of the detector graph \mathcal{D} is also d . Hence the protocol underlying D implements a fault-tolerant logical measurement.

To understand the code distance of \mathcal{G}_X , we must analyze how the existing logical operators could change in shape after fusing the ancilla patch. We begin with Z -type logical operators, whose weight does not depend on L .

Theorem 3. *Each nontrivial logical Z operator in \mathcal{G}_X has weight at least d .*

Proof. Suppose P is a Z operator that commutes with the stabilizer of \mathcal{G}_X . We need to show that P is either weight at least d or is a product of Z checks. Consider the the restriction of P to the qubits \mathcal{V} of the code \mathcal{G} , written $P|_{\mathcal{V}}$. $P|_{\mathcal{V}}$ commutes with all X checks of the original code \mathcal{G} and is therefore a logical operator of that code. Assuming it is not in the stabilizer, its weight is at least d which implies the weight of P is also at least d . On the other hand, suppose $P|_{\mathcal{V}}$ is a product of Z checks of the original code. This implies P can be multiplied by a product of Z checks from \mathcal{G}_X to obtain an operator S supported entirely on the interface and module qubits $(C_1 \cup C_3 \cup \dots \cup C_L) \cup (V_2 \cup V_4 \cup \dots \cup V_{L-1})$. Notably, S is equal to P modulo stabilizers from \mathcal{G}_X . We denote the support of S with $c_j \in C_j$ for odd j and $v_i \in V_i$ for even i , allowing us to write

$$S = \prod_{\substack{j=1 \\ j \text{ odd}}}^L Z(c_j \in C_j) \cdot \prod_{\substack{i=2 \\ i \text{ even}}}^{L-1} Z(v_i \in V_i), \quad (3)$$

recalling notation from section 2.1. Because S commutes with all $X(V_L)$, we must have $c_L F = v_{L-1}$. Similarly, because of commutation with checks in V_j for all odd $j < L$ we have $c_j F = v_{j-1} + v_{j+1}$. Finally, because of commutation with checks in V_1 , $c_1 F = v_2$. Adding all these equations together modulo two results in the right-hand sides telescoping down to zero. If we define $c_{\text{tot}} = c_1 + c_3 + \dots + c_L$, we find $c_{\text{tot}} F = 0$. Because rows of G span the row nullspace of F , there exists r such that $rG = c_{\text{tot}}$ and $\mathcal{H}_Z(r \in U_L) = Z(c_{\text{tot}} \in C_L)$.

We can multiply S by checks $\mathcal{H}_Z(c_1 \in C_2)\mathcal{H}_Z(c_1 + c_3 \in C_4) \dots \mathcal{H}_Z(c_1 + c_3 + \dots + c_{L-2} \in C_{L-1})$ to obtain

$$S' = Z(c_{\text{tot}} \in C_L) \prod_{\substack{i=2 \\ i \text{ even}}}^{L-1} Z(v'_i \in V_i) = \mathcal{H}_Z(r \in U_L) \prod_{\substack{i=2 \\ i \text{ even}}}^{L-1} Z(v'_i \in V_i) := \mathcal{H}_Z(r \in U_L) S'', \quad (4)$$

where v'_i are some vectors that can be determined in terms of c_j and v_i . However, S'' must therefore commute with all X checks while being supported only on $V_2 \cup V_4 \cup \dots \cup V_{L-1}$. It is easy to see this implies $S'' = I$ and so S' and S are products of Z checks in \mathcal{G}_X . \square

Ensuring that the X operators have high weight requires selecting L . The best choice of L depends on the nature of the induced Tanner graph determined by \bar{X}_M . We derive a sufficient condition in terms of the *boundary Cheeger constant* of the induced Tanner graph, which has adjacency matrix F .

Definition 4 (Boundary Cheeger Constant). For a bipartite graph $F^\top : V \rightarrow C$ and a set of vertices $v \subset V$, define the *boundary* $\partial v \subset C$ to be the set of vertices with an odd number of neighbors in v . In terms of indicator vectors, we may write $\partial v = vF^\top$. The *boundary Cheeger constant* of a Tanner graph is defined as

$$\beta = \min_{v \subset V, |v| \leq |V|/2} |\partial v|/|v|. \quad (5)$$

The fact that \bar{X}_M is a logical operator implies a condition on the support of other logical operators.

Lemma 5. Suppose \bar{X} is a logical X operator (inequivalent to \bar{X}_M) supported on $v \subset \mathcal{V}$. Then $|v \setminus V_0| + |V_0 \setminus v| \geq d$.

Proof. Notice $\bar{X}_M \bar{X}$, which is supported on $(v \setminus V_0) \cup (V_0 \setminus v)$, is also a nontrivial logical operator, and therefore has weight at least d . \square

This observation lets us bound the minimum distance in terms of L and the boundary Cheeger constant.

Theorem 6. If the induced Tanner graph of \bar{X}_M is $F : C_0 \rightarrow V_0$, suppose $F^\top : V_1 \rightarrow C_1$ has boundary Cheeger constant β . If \mathcal{G}_X is constructed with L layers such that $\lceil L/2 \rceil \geq 1/\beta$, then the code \mathcal{G}_X has distance at least d .

Proof. Theorem 3 bounds the minimum weight of Z -type logical operators in \mathcal{G}_X for all L . Only the logical X operators remain to be bounded.

Any X -type logical operator of code \mathcal{G} is still a logical operator of the merged code \mathcal{G}_X . Irreducibility of \bar{X}_M implies that this set of logical X -type operators provides a complete basis of X -type logical operators of the $k-1$ qubit code \mathcal{G}_X . Hence, consider any nontrivial X -type logical operator P of \mathcal{G}_X supported entirely on \mathcal{V} . It is also a logical operator of \mathcal{G} so it has weight at least d . We will show P cannot be reduced in weight to below d by multiplying by the X -checks of \mathcal{G}_X .

Let $P = X(t \in \mathcal{V})$ be an X -type logical operator of \mathcal{G}_X . Consider

$$P' = P \prod_{\substack{j=1 \\ j \text{ odd}}}^L \mathcal{H}_X(v_j) = X(t + v_1 \in \mathcal{V}) \prod_{\substack{j=1 \\ j \text{ odd}}}^L X(v_j F^\top \in C_j) \prod_{\substack{i=3 \\ i \text{ odd}}}^L X(v_i + v_{i-2} \in V_{i-1}), \quad (6)$$

for arbitrary v_j indicating multiplication by an arbitrary combination of checks from the ancilla system. The definition of Cheeger's constant says that $|v_j F^\top| \geq \beta \min(|v_j|, |V_0| - |v_j|)$, and it follows that

$$|P'| \geq |t + v_1| + \sum_{\substack{j=1 \\ j \text{ odd}}}^L \beta \min(|v_j|, |V_0| - |v_j|) + \sum_{\substack{i=3 \\ i \text{ odd}}}^L |v_i + v_{i-2}|, \quad (7)$$

$$\geq \sum_{\substack{j=1 \\ j \text{ odd}}}^L \left[\frac{1}{\lceil L/2 \rceil} \left(|t + v_1| + \sum_{\substack{i=3 \\ i \text{ odd}}}^j |v_i + v_{i-2}| \right) + \beta \min(|v_j|, |V_0| - |v_j|) \right] \quad (8)$$

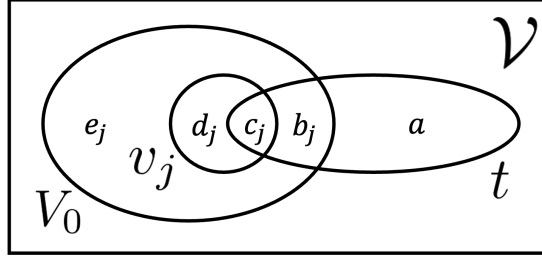


Figure 4: Notation describing the intersection of supports of objects in the proof of Theorem 6. Here \mathcal{V} is the set of all qubits in the original code \mathcal{G} , V_0 is the support of the logical X operator being measured, $t \in \mathcal{V}$ describes the support of another logical X operator P , and v_j describes a set of checks from V_j multiplying P . Letters a, b_j, c_j, d_j, e_j denote the sizes of the sets in which they are drawn.

where the second inequality follows by removing some fraction of the $|v_j + v_{j-2}|$ terms and rearranging. By repeated use of the triangle inequality, the parenthesized term is at least $|t + v_j|$, so

$$|P'| \geq \sum_{\substack{j=1 \\ j \text{ odd}}}^L \left[\frac{1}{\lceil L/2 \rceil} |t + v_j| + \beta \min(|v_j|, |V_0| - |v_j|) \right] \quad (9)$$

$$\geq \frac{1}{\lceil L/2 \rceil} \sum_{\substack{j=1 \\ j \text{ odd}}}^L \left[|t + v_j| + \min(|v_j|, |V_0| - |v_j|) \right], \quad (10)$$

with the second inequality making use of $\beta \lceil L/2 \rceil \geq 1$.

Now to complete the proof of $|P'| \geq d$ it is sufficient to show $|t + v_j| + \min(|v_j|, |V_0| - |v_j|) \geq d$ for all j . Using the notation of Figure 4, we need $(a + b_j + d_j) + \min(c_j + d_j, b_j + e_j) \geq d$ or, equivalently, both

$$a + b_j + c_j + 2d_j \geq d \quad \text{and} \quad a + 2b_j + d_j + e_j \geq d. \quad (11)$$

Note that both $X(t \in \mathcal{V})$ and $X(t \in \mathcal{V})X(V_0)$ are logical operators of the original code \mathcal{G} and thus each has weight at least d . Translated to the notation of Figure 4, this means $a + b_j + c_j \geq d$ and $a + d_j + e_j \geq d$, which in turn imply (11). \square

Next we analyze the detector graph \mathcal{D} described in Section 3.2 and give lower bounds on fault distance. For our purposes it makes sense to analyze two different fault distances: the *logical* fault distance and the *measurement* fault distance. These are defined similarly to fault distance in [BHK24].

Definition 7. Consider a phenomenological noise model on the detector graph \mathcal{D} : Pauli errors can occur on qubits in between any rounds of measurement, and any measurement outcome can be faulty. We say a detector *triggers* when the associated parity between measurement outcomes is 1, and we say an error is *undetected* if it triggers no detectors. The *measurement fault distance* is the minimum weight of an undetected error that causes an error in the measurement outcome. The *logical fault distance* is the minimum weight of an undetected error that causes a logical Pauli error on a qubit in \mathcal{G} other than the measured qubit and does not cause a measurement error.

Our proof uses the idea that code switching using Pauli measurements can be analyzed in terms of subsystem codes [VLC⁺19]. Let \bar{Z}_M be the symplectic partner to \bar{X}_M , \hat{e}_l denote a basis vector, $C_1^{\text{sep}} = \{Z(\hat{e}_l \in C_1) : l \in C_1\}$ denote the set of all single qubit Pauli Z operators on the qubits C_1 , and \mathcal{C}_0^Z be checks in \mathcal{C}^Z that are not supported on V_0 . We also let $V_j \text{ odd} = V_1 \cup V_3 \cup \dots \cup V_L$ and $C_i \text{ even} = C_0 \cup C_2 \cup \dots \cup C_{L-1}$. Consider the stabilizer group of the merged code \mathcal{G}_X

$$\mathcal{S}_X = \langle C^X, \mathcal{C}_0^Z, V_j \text{ odd}, C_i \text{ even}, U_L \rangle, \quad (12)$$

and the stabilizer group of the original code, interface qubits in $|0\rangle$, and module, with or without \bar{X}_M included

$$\mathcal{S} = \langle C^X, \mathcal{C}_0^Z, V_{j \geq 3 \text{ odd}}, C_i \text{ even}, C_1^{\text{sep}} \rangle, \quad \mathcal{S}' = \langle \mathcal{S}, \bar{X}_M \rangle. \quad (13)$$

Note $U_L \subseteq \mathcal{S}$ as written even though it is not explicitly included. Also consider the gauge group

$$\mathcal{U} = \langle C^X, \mathcal{C}_0^Z, V_{j \text{ odd}}, C_i \text{ even}, C_1^{\text{sep}} \rangle = \langle \mathcal{S}, \mathcal{S}_X \rangle. \quad (14)$$

These groups satisfy the subgroup relations

$$\mathcal{S}' \leq \mathcal{U}, \quad \mathcal{S}_X \leq \mathcal{U}. \quad (15)$$

In particular, \mathcal{S}' and \mathcal{S}_X are two different ways of fixing the gauge of \mathcal{U} to get stabilizer codes.

All three codes corresponding to \mathcal{S}' , \mathcal{S}_X , and \mathcal{U} have $k - 1$ logical qubits and a logical basis for each can be chosen to consist of the same set of operators $\mathcal{L} = \langle \bar{X}_i, \bar{Z}_i : i = 1, \dots, k - 1 \rangle$. To see this, note that any logical X operator \bar{X}_i (inequivalent to \bar{X}_M) of \mathcal{S} on the original code qubits is still a logical operator of each of the three codes. Also, if \bar{Z}'_i is a nontrivial logical Z operator of \mathcal{S} that commutes with \bar{X}_M , then we claim it can be multiplied by stabilizers of the original code to obtain an equivalent \bar{Z}_i suitable for inclusion in \mathcal{L} because it has no support on V_0 . This statement is a corollary of the following lemma.

Lemma 8. *Suppose \bar{X}_M is irreducible. Then for any vector v with even weight supported on V_0 , there exists a vector c supported on C_0 such that $cF = v$.*

Proof. Since the only nonzero column vector w such that $Fw = 0$ is the all 1s vector, the rows of F must span the checks of a classical repetition code. Any vector of even weight can be expressed as a linear combination of rows of F since the checks of a repetition code generate all vectors of even weight. \square

We also use $\mathcal{L}^* = \mathcal{L} \setminus \{I\}$ to denote the nontrivial logical operators.

For Pauli p and sets of Pauli operators \mathcal{T} and \mathcal{T}' , let $p\mathcal{T} = \{pq : q \in \mathcal{T}\}$ and $\mathcal{T}\mathcal{T}' = \{pq : p \in \mathcal{T}, q \in \mathcal{T}'\}$. Also, let $d(\mathcal{T})$ be the minimum weight of any Pauli in \mathcal{T} . Then the code distances of codes \mathcal{S}' , \mathcal{S}_X , and \mathcal{U} are written $d(\mathcal{L}^*\mathcal{S}')$, $d(\mathcal{L}^*\mathcal{S}_X)$, and $d(\mathcal{L}^*\mathcal{U})$, respectively, and because of Eq. (15),

$$d(\mathcal{L}^*\mathcal{U}) \leq d(\mathcal{L}^*\mathcal{S}_X), \quad d(\mathcal{L}^*\mathcal{U}) \leq d(\mathcal{L}^*\mathcal{S}'), \quad d(\bar{Z}_M \mathcal{L} \mathcal{U}) \leq d(\bar{Z}_M \mathcal{L} \mathcal{S}'). \quad (16)$$

As the ‘‘weakest’’ code out of the three, \mathcal{U} and its code distance ends up determining the logical and measurement fault distances of our protocol. Let R be the number of rounds we measure the checks of the merged code.

Lemma 9. *The measurement fault distance of the X system is $\min(R, d(\bar{Z}_M \mathcal{L} \mathcal{U}))$. The logical fault distance of the X system is $d(\mathcal{L}^*\mathcal{U})$.*

Proof. We denote by \mathcal{M}_t the (abelian) group of Paulis generated by the checks measured in timestep t . In particular, $\mathcal{M}_0 = \mathcal{S} = \mathcal{M}_{R+1}$ measures the original code, interface qubits in $|0\rangle$, and module (see the top and bottom of Figure 3). For $0 < t < R + 1$, \mathcal{M}_t measures the merged code stabilizers \mathcal{S}_X .

Measurement differences are denoted $\mathcal{M}_{t \rightarrow t'} = \mathcal{M}_t \cap \mathcal{M}_{t'}$ for $t' > t$. Each element of a detector group $\mathcal{M}_{t \rightarrow t'}$ is indeed a detector because, given its value at time t , in the absence of errors it will have the same value at time t' . The explicit parities \mathcal{D}_t described in Section 3.2 suffice to indicate which detectors in $\mathcal{M}_{t \rightarrow t+1}$ changed from t to $t+1$. While the $\mathcal{M}_{t \rightarrow t+1}$ are a generating set of detectors sufficient for decoding, it is also true that an undetected error in the sense of Definition 7 should be undetected by (i.e. commute with) any detector group $\mathcal{M}_{t \rightarrow t'}$. This means that undetected errors are elements of the centralizer $\mathcal{C}(\mathcal{M}_{t \rightarrow t'})$.

Detector groups $\mathcal{M}_{t \rightarrow t'}$ fall into three cases. If $t = 0$ and $0 < t' < R + 1$ or $0 < t < R + 1$ and $t' = R + 1$, then $\mathcal{M}_{t \rightarrow t'} = \mathcal{S} \cap \mathcal{S}_X$, the stabilizers that are both in the original code and merged code. If $0 < t, t' < R + 1$, then $\mathcal{M}_{t \rightarrow t'} = \mathcal{S}_X$, the merged code stabilizers. Finally, if $t = 0$ and $t' = R + 1$, then $\mathcal{M}_{0 \rightarrow R+1} = \mathcal{S}$, the original code stabilizers.

We assume that the final round is free of measurement errors to disallow hiding detectors at the future time boundary. Presumably this strategy would be unsuccessful anyway since it would be detected by future $t > R + 1$ measurements. Because the final round is perfect, any qubit errors must at this point amount to an undetectable error. We point out that an ideal round of measurement is also done in our numerical case study (see Section 4) at $t = R + 2$ for the same reason.

If some nontrivial Pauli error P occurred on the qubits we will bound its weight. Such a Pauli error is necessary to cause a logical fault and is one way to cause a measurement fault. The other way to cause a measurement fault is with only measurement errors. Because we repeat the measurement of \mathcal{S}_X (which contains \bar{X}_M) R times, this way to cause a measurement fault requires at least R measurement errors.

Let t be the latest time before the first qubit error, and t' be the earliest time after the last qubit error, so that by time t' the accumulated qubit error is P . Hiding this error from detection with measurement errors in steps t' and later will fail due to the perfect measurement round at $R + 1$. Thus, P must commute with all detectors in $\mathcal{M}_{t \rightarrow t'}$ (although it may also require measurement errors at times between $t + 1$ and $t' - 1$ to avoid detection at those times). Given the discussion above, this means P is in the centralizer of $\mathcal{S} \cap \mathcal{S}_X$, \mathcal{S}_X , or \mathcal{S} depending on t and t' .

We provide generating sets of these centralizers so we can see exactly which elements lead to logical or measurement faults using Definition 7. We deal with the three cases one at a time. First,

$$\mathcal{C}(\mathcal{S} \cap \mathcal{S}_X) = \left\langle \begin{array}{c} \mathcal{S} \cap \mathcal{S}_X \\ V_1 \\ C_1^{\text{sep}} \end{array} \quad \begin{array}{c} \bar{X}_M \\ \bar{Z}_M \end{array} \quad \begin{array}{c} \bar{X}_{i=1,\dots,k-1} \\ \bar{Z}_{i=1,\dots,k-1} \end{array} \right\rangle. \quad (17)$$

The elements highlighted in gray are a generating set of \mathcal{U} and the \bar{X}_i and \bar{Z}_i in the last column are the generators of \mathcal{L} . A measurement fault is an element of $\mathcal{C}(\mathcal{S} \cap \mathcal{S}_X)$ that includes \bar{Z}_M , the only generator of $\mathcal{C}(\mathcal{S} \cap \mathcal{S}_X)$ that anticommutes with \bar{X}_M . So measurement faults are exactly the elements of $\bar{Z}_M \mathcal{L} \mathcal{U}$. Similarly, logical faults are elements of $\mathcal{C}(\mathcal{S} \cap \mathcal{S}_X)$ that do not include \bar{Z}_M (since Definition 7 specifies that logical faults do not flip the logical measurement) and include at least one of \bar{X}_i or \bar{Z}_i . Thus, logical faults are exactly the elements of $\mathcal{L}^* \mathcal{U}$.

Second,

$$\mathcal{C}(\mathcal{S}_X) = \left\langle \begin{array}{c} \mathcal{S}_X \\ \bar{Z}_{i=1,\dots,k-1} \end{array} \right\rangle. \quad (18)$$

In this case, it is not possible to get a measurement fault, because $\bar{X}_M \in \mathcal{S}_X$ is a detector. Similar to the first case, logical faults are exactly the elements of $\mathcal{L}^* \mathcal{S}_X$.

Third,

$$\mathcal{C}(\mathcal{S}) = \left\langle \begin{array}{c} \mathcal{S} \\ \bar{Z}_M \end{array} \quad \begin{array}{c} \bar{X}_M \\ \bar{Z}_M \end{array} \quad \begin{array}{c} \bar{X}_{i=1,\dots,k-1} \\ \bar{Z}_{i=1,\dots,k-1} \end{array} \right\rangle. \quad (19)$$

The highlighted elements are generators of \mathcal{S}' . Similar to above, measurement faults are exactly elements of $\bar{Z}_M \mathcal{L} \mathcal{S}'$ and logical faults are exactly elements of $\mathcal{L}^* \mathcal{S}'$.

Therefore, combining the three cases we see that the logical fault distance is at least

$$\min(d(\mathcal{L}^* \mathcal{S}'), d(\mathcal{L}^* \mathcal{U}), d(\mathcal{L}^* \mathcal{S}_X)) = d(\mathcal{L}^* \mathcal{U}), \quad (20)$$

where we used Eq. (16). The logical fault distance is exactly $d(\mathcal{L}^* \mathcal{U})$ because an error from $\mathcal{L}^* \mathcal{U}$ can happen between \mathcal{M}_0 and \mathcal{M}_1 without necessitating any measurement errors to hide it from detection.

Similarly, combining the three cases with the case of R measurement errors we find the measurement fault distance is at least $\min(R, d(\bar{Z}_M \mathcal{L} \mathcal{S}'), d(\bar{Z}_M \mathcal{L} \mathcal{U})) = \min(R, d(\bar{Z}_M \mathcal{L} \mathcal{U}))$, again using Eq. (16). Again, this is exactly the measurement fault distance because all qubit errors could occur between \mathcal{M}_0 and \mathcal{M}_1 . \square

Though we proved it in the special case of measuring \bar{X}_M for simplicity, this lemma can be generalized to apply to any of the ancilla measurement schemes in this paper. There is always an original stabilizer group \mathcal{S}_O and merged code group \mathcal{S}_M measured $R \geq 1$ times. Let $\mathcal{U} = \langle \mathcal{S}_O, \mathcal{S}_M \rangle$. If \bar{P}_M is the logical operator being measured, let \bar{Q}_M be a Pauli that anticommutes with it. We can establish a group of logical operators

for $k-1$ qubits \mathcal{L} that is the same for all the codes, and such that elements of \mathcal{L} commute with both \bar{P}_M and \bar{Q}_M . The lemma then applies with \bar{Q}_M replacing \bar{Z}_M . For instance, if we are measuring $\bar{P}_M = \bar{X}_1 \bar{X}_2$ as in the next section, we can take $\bar{Q}_M = \bar{Z}_1$, set up $\mathcal{L} = \langle \bar{X}_2, \bar{Z}_1 \bar{Z}_2, \bar{X}_i, \bar{Z}_i, \forall i = 3, \dots, k \rangle$, and calculate $d(\bar{Q}_M \mathcal{L} \mathcal{U})$ and $d(\mathcal{L}^* \mathcal{U})$ to bound the measurement and logical fault distances.

However, when we measure X -type (or, symmetrically, Z -type) operators on a CSS code, we can be more specific about the fault distances in Lemma 9. We say a Pauli is X -type (resp. Z -type) if it acts as either I or X (resp. Z) on all qubits. Let $d_X(\mathcal{T})$ and $d_Z(\mathcal{T})$ indicate the lowest weight of any X - or Z -type operator in Pauli set \mathcal{T} , respectively. Then we have the following lemma for the case of measuring \bar{X}_M .

Lemma 10. *With \mathcal{S} , \mathcal{S}_X , \mathcal{U} , and \mathcal{L} defined above for the X ancilla system, $d(\mathcal{L}^* \mathcal{U}) = \min(d_Z(\mathcal{L}^* \mathcal{S}), d_X(\mathcal{L}^* \mathcal{S}_X))$ and $d(\bar{Z}_M \mathcal{L} \mathcal{U}) = d_Z(\bar{Z}_M \mathcal{L} \mathcal{S})$.*

Proof. Since \mathcal{U} and \mathcal{L} are generated by only X - and Z -type Paulis (i.e. they are CSS) and \bar{Z}_M is Z -type,

$$d(\mathcal{L}^* \mathcal{U}) = \min(d_Z(\mathcal{L}^* \mathcal{U}), d_X(\mathcal{L}^* \mathcal{U})) \quad \text{and} \quad d(\bar{Z}_M \mathcal{L} \mathcal{U}) = d_Z(\bar{Z}_M \mathcal{L} \mathcal{U}). \quad (21)$$

Now note that the Z -type operators of \mathcal{U} are exactly the same group of Z -type operators in \mathcal{S} , and so $d_Z(\mathcal{L}^* \mathcal{U}) = d_Z(\mathcal{L}^* \mathcal{S})$ and $d(\bar{Z}_M \mathcal{L} \mathcal{U}) = d_Z(\bar{Z}_M \mathcal{L} \mathcal{S})$. Likewise, the X -type operators of \mathcal{U} are the same group as the X -type operators of \mathcal{S}_X , and so $d_X(\mathcal{L}^* \mathcal{U}) = d_X(\mathcal{L}^* \mathcal{S}_X)$. \square

In particular, if the original code has code distance d , then $d_Z(\mathcal{L}^* \mathcal{S}) \geq d$ and $d_Z(\bar{Z}_M \mathcal{L} \mathcal{S}) \geq d$ are automatic. Thus, Lemmas 9 and 10 combine to show the fault distance of the X ancilla system is large provided the merged code \mathcal{S}_X has large X distance.

Theorem 11. *Let d be the distance of the original code. If the stabilizers of the merged code are measured at least d times, the measurement fault distance of the X system is at least d . If the merged code has X distance at least d (e.g. satisfies Theorem 6), the logical fault distance of the X system is also at least d .*

We note that initializing the module code on qubits $V_{i \geq 2 \text{ even}} \cup C_{j \geq 3 \text{ odd}}$ was used in our \bar{X}_M measurement protocol just to make a specific choice of codes at the merge and split steps. This is flexible to some extent. For instance, one could instead initialize all qubits $V_{i \geq 2 \text{ even}} \cup C_{j \geq 1 \text{ odd}}$ to $|0\rangle$ and make the same arguments to arrive at Lemma 9 and Theorem 11. The key property we need from a choice of initialization is that the Z checks are reliable at the merge and split.

3.4 Modular Decoder Achieving Measurement Fault-Distance

Above we showed that the phenomenological fault-distances of the decoding graph \mathcal{D} are d for both measurement errors and logical errors whenever it is constructed with at least $R \geq d$ rounds. To ensure practicality of the scheme we must also ensure that a decoder can correct errors of weight $< d/2$. It is reasonable to assume that such a decoder already exists for the code \mathcal{G} on its own. In this section we show that if there is a good decoder for the original code \mathcal{G} , then there also exists a good decoder for extracting measurement outcomes from the measurement protocol specified by \mathcal{D} .

Since \mathcal{G} and \mathcal{G}_X are CSS codes, X and Z errors (and Z and X measurement errors) can be decoded separately. Since the measurement outcome is only affected by Z errors (and X measurement errors), we restrict our attention to these errors specifically.

We divide the parity checks in \mathcal{D} into two parts. $\mathcal{D}^{\mathcal{G}}$ contains the detectors on \mathcal{C}^X , the X checks of the original code \mathcal{G} . \mathcal{D}^{anc} contains the checks on the remaining X checks of \mathcal{G}_X corresponding to vertices V_j for odd j . We consider a modular approach where we first run a given decoder on $\mathcal{D}^{\mathcal{G}}$ only, and propagate the resulting corrections to the X checks in \mathcal{D}^{anc} . We show that there exists a decoder for decoding the remaining errors in \mathcal{D}^{anc} that cannot result in a correction that flips the measurement outcome unless the error has weight $\geq d/2$.

The measured observable \bar{X} is the product of all X checks in \mathcal{G}_X . Hence an error that flips the measurement outcome must flip an odd number of X checks. Indeed, errors that flip an even number of checks can be identified using Lemma 8.

The main idea is to reduce decoding to a matching problem on a chain, where every node in the chain corresponds to a step in \mathcal{D}^{anc} . Since errors that flip an even number of X -checks within a round of measurements cannot affect the measurement outcome, we can restrict our attention to the total parity of the detectors within each step. Then the matching decoder is the only part of the decoding algorithm that could introduce a measurement error. It is well-known that a matching decoder on a line of length R can only fail to correct an error if the error has weight $\geq R/2$, which is $\geq d/2$ since $R \geq d$.

Theorem 12. *Suppose there exists a decoder that, for any collection $E_{\mathcal{G}}$ of Z -qubit and X -measurement errors of weight $< d/2$ in the detector graph $\mathcal{D}^{\mathcal{G}}$, outputs a correction $E'_{\mathcal{G}}$ consisting of Z -qubit errors and X -measurement errors consistent with the detectors and equivalent to $E_{\mathcal{G}}$ up to the stabilizers of \mathcal{G} .*

Then there exists a decoder for \mathcal{D} as a whole that outputs a correction E' such that, if the true error is E of weight $< d/2$, the product EE' triggers no detectors and commutes with the measured observable \bar{X}_M .

Proof. The decoder operates as follows. First we run the provided decoder on $\mathcal{D}^{\mathcal{G}}$ to obtain the correction $E'_{\mathcal{G}}$. The Z errors in $E'_{\mathcal{G}}$ may affect some X -checks on V_0 . We flip the associated detectors in \mathcal{D}^{anc} , so that the detector values in \mathcal{D}^{anc} only indicate Z -qubit errors a X -measurement errors on the interface and module.

Consider the steps $\mathcal{D}_1^{\text{anc}}, \mathcal{D}_2^{\text{anc}}, \dots, \mathcal{D}_R^{\text{anc}}$. We call a step $\mathcal{D}_i^{\text{anc}}$ *odd* if an odd number of detectors trigger, and *even* otherwise. Now we solve a matching problem on a line: the odd steps are sorted into adjacent pairs, possibly involving the endpoints of the sequence. In particular, suppose $\mathcal{D}_{j_1}^{\text{anc}}, \mathcal{D}_{j_2}^{\text{anc}}, \dots, \mathcal{D}_{j_k}^{\text{anc}}$ are the odd steps with $j_1 < j_2 < \dots < j_k$. If k is even then the two possible matchings are:

$$(\mathcal{D}_{j_1}^{\text{anc}}, \mathcal{D}_{j_2}^{\text{anc}}), (\mathcal{D}_{j_3}^{\text{anc}}, \mathcal{D}_{j_4}^{\text{anc}}), \dots, (\mathcal{D}_{j_{k-1}}^{\text{anc}}, \mathcal{D}_{j_k}^{\text{anc}}), \quad (22)$$

$$(\text{start}, \mathcal{D}_{j_1}^{\text{anc}}), (\mathcal{D}_{j_2}^{\text{anc}}, \mathcal{D}_{j_3}^{\text{anc}}), \dots, (\mathcal{D}_{j_k}^{\text{anc}}, \text{end}). \quad (23)$$

and if k is odd, the two possible matchings are:

$$(\mathcal{D}_{j_1}^{\text{anc}}, \mathcal{D}_{j_2}^{\text{anc}}), (\mathcal{D}_{j_3}^{\text{anc}}, \mathcal{D}_{j_4}^{\text{anc}}), \dots, (\mathcal{D}_{j_k}^{\text{anc}}, \text{end}), \quad (24)$$

$$(\text{start}, \mathcal{D}_{j_1}^{\text{anc}}), (\mathcal{D}_{j_2}^{\text{anc}}, \mathcal{D}_{j_3}^{\text{anc}}), \dots, (\mathcal{D}_{j_{k-1}}^{\text{anc}}, \mathcal{D}_{j_k}^{\text{anc}}). \quad (25)$$

We select the matching that minimizes the length between paired steps. For example, the lengths of the matchings when k is odd are $(j_2 - j_1) + (j_4 - j_3) + (R - j_k)$, and $(j_1 - 0) + (j_2 - j_1) + (j_k - j_{k-1})$ respectively.

We now identify errors in E' that cause each pair of odd steps $(\mathcal{D}_j^{\text{anc}}, \mathcal{D}_k^{\text{anc}})$ to become even. We select any single X -check in V_1 and insert measurement errors for all measurements in between the two steps. Inserting such errors flips one detector each in $\mathcal{D}_j^{\text{anc}}$ and $\mathcal{D}_k^{\text{anc}}$, making them even, while keeping the steps in between identical. A similar process works for $(\text{start}, \mathcal{D}_{j_1}^{\text{anc}})$ and $(\mathcal{D}_{j_k}^{\text{anc}}, \text{end})$ pairs since flipping a V_1 measurement result in the first or final round of measurements only affects detector steps $\mathcal{D}_1^{\text{anc}}$ and $\mathcal{D}_R^{\text{anc}}$ respectively.

After introducing the above errors, all the steps are even. However, a particular even step may still feature an odd number of triggered detectors within each group of X -check vertices V_j for odd j . Since the step itself is even, there must be an even number of such odd groups. Z -qubit errors on V_i for even i in that layer flip pairs of detectors based on V_j checks within one step. Hence we can find a choice of such Z -errors that cause all groups of X -checks on V_j for odd j to be even.

To finish the decoding, we leverage Lemma 8 to identify Z errors on each C_j for odd j that flip the corresponding X checks on V_j . We return the product of all identified errors and $E'_{\mathcal{G}}$ as E' for \mathcal{D} as a whole. Since inserting these errors untriggered all detectors, the product EE' must trigger no detectors.

Suppose the true error on \mathcal{D} was E of weight $< d/2$. It remains to show that EE' commutes with the measured observable \bar{X} . \bar{X} is the product of all the X -checks on V_j for odd j . Here we point out that several parts of E introduced above do not affect the measurement result. Hence a worst-case error E does not feature these parts, since they needlessy increase the weight. This lets us restrict our attention to corrections E of a certain form. Since $E_{\mathcal{G}}E'_{\mathcal{G}}$ is equivalent to the identity up to the stabilizer of \mathcal{G} by assumption, we can restrict our attention to an error E of weight $< d/2$ supported on \mathcal{D}^{anc} only. Furthermore, since the errors identified from Lemma 8 flip an even number of X -checks in any V_j for odd j , these must commute with

\bar{X} as well. So we may furthermore assume that E flips at most one detector for each V_j within each layer. Similarly, flipping an even number of bits within the odd V_j groups within an even layer also commutes with the measurement outcome, so we can assume that errors only occur on V_1 .

So the only part of the decoding process that could cause EE' to flip the measurement outcome is the matching problem. Measurement errors on V_1 introduced as part of E' could form a chain of errors within EE' connecting the first round to the final round. Then EE' triggers no detectors but flips the logical measurement outcome. Suppose EE' is as such. Observe that the sum of the distances between paired layers for the two possible matchings is R , for both the even and odd k case. That means that one of them has length $\leq R/2$ and the other one $\geq R/2$. Since the decoder always picks the shorter matching, it will always pick one of length $\leq R/2$. For EE' to form the entire chain, E must then correspond to the matching of length $\geq R/2$. \square

We observe that if every qubit in C_1 is adjacent to exactly two checks from V_1 , then we can simply use a minimum-weight perfect matching (MWPM) decoder on \mathcal{D}^{anc} . This condition is equivalent to every Z -check in C_0 touching two qubits in V_0 . This is not true for arbitrary codes and logical operators. However, in our case study on the $\llbracket 144, 12, 12 \rrbracket$ code in Section 4, we find logical operators where this condition is satisfied.

3.5 Joint X Measurement

In this section, given ancilla systems for measuring two logical X operators \bar{X}_1 and \bar{X}_2 that do not share support, we present a method to measure the joint operator $\bar{X}_1\bar{X}_2$ by connecting the two systems. For instance, this joint system can be used to connect two distinct codeblocks provided they are each equipped with an ancilla system, and in this case, we prove that the fault and code distances of the joint system are the minimum of the distances of the individual systems. If \bar{X}_1 and \bar{X}_2 do share support, then $\bar{X}_1\bar{X}_2$ is best measured with an X ancilla system as described in Section 3.1.

Our method of joint measurement is distinct from the proposal in [CKBB22], not just from the fact that our ancilla systems are gauge-fixed, but also because their approach actually requires $2d - 1$ layers to preserve the code distance and, more specifically, to preserve the weight of \bar{X}_1 or \bar{X}_2 , which are still logical operators in the merged code. Instead of more layers, we introduce a collection of $\min(|\bar{X}_1|, |\bar{X}_2|)$ qubits that are connected to X checks in both ancilla systems. We term these qubits *bridge* qubits. The joint system is depicted in Figure 5.

To describe how the bridge qubits are connected, we need to establish notation distinguishing the two ancilla systems for measuring \bar{X}_1 and \bar{X}_2 individually. Generally, we keep the notation from Figure 2, but we superscript sets of qubits and checks by (1) or (2). The collection of bridge qubits are indicated by B and a new set of gauge checks that act on bridge qubits is denoted U^B . See again Figure 5.

Suppose j_1 and j_2 are any odd integers, each specifying a particular layer from the \bar{X}_1 and \bar{X}_2 systems respectively. Each bridge qubit is checked by one check from $V_{j_1}^{(1)}$ and one check from $V_{j_2}^{(2)}$. To specify connections between checks $V_{j_1}^{(1)}$ and qubits B , we need only give a binary matrix $S^{(1)}$ with exactly one 1 per column (each bridge qubit is connected to some check) and at most one 1 per row (checks are connected to at most one bridge qubit). A similar matrix $S^{(2)}$ specifies how $V_{j_2}^{(2)}$ and B are connected. Since $|B| = \min(|\bar{X}_1|, |\bar{X}_2|) = \min(|V_{j_1}^{(1)}|, |V_{j_2}^{(2)}|)$, at least one of $S^{(1)}$, $S^{(2)}$ is a square matrix with exactly one 1 per row and column.

The next lemma characterizes the additional gauge operators introduced by including the bridge.

Lemma 13. *A complete, linearly independent basis of gauge checks of U^B in the joint ancilla system consists of $|B| - 1$ checks. Moreover, there is a basis in which each check acts on exactly two bridge qubits.*

Proof. Define a matrix specifying connectivity between checks in sets $V_{j_1}^{(1)}$ and $V_{j_2}^{(2)}$ and qubits in sets $C_{j_1}^{(1)}$, $C_{j_2}^{(2)}$, and B .

$$G = \begin{pmatrix} F^{(1)\top} & 0 & S^{(1)} \\ 0 & F^{(2)\top} & S^{(2)} \end{pmatrix}. \quad (26)$$

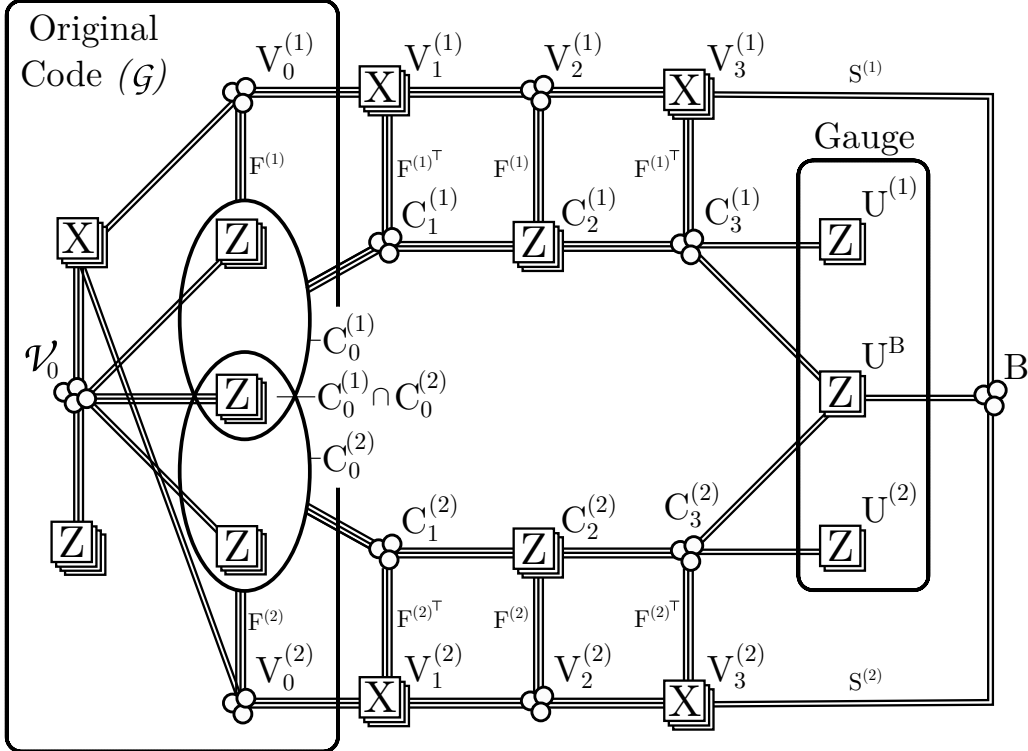


Figure 5: The ancilla system for measuring the joint logical operator $\bar{X}_1 \bar{X}_2$, where $\text{supp } \bar{X}_1 = V_0^{(1)}$ and $\text{supp } \bar{X}_2 = V_0^{(2)}$ are disjoint. The joint system is exactly the two systems for measuring \bar{X}_1 and \bar{X}_2 with the addition of bridge qubits B and gauge checks U^B . Checks in $C_0^{(1)} \cap C_0^{(2)}$ are each connected to two ancilla qubits, one from $C_1^{(1)}$ and one from $C_1^{(2)}$. Although not strictly necessary, the drawing assumes that the number of layers in the \bar{X}_1 and \bar{X}_2 systems are the same and the bridge connects the last layers together. In general, the bridge B can be used to connect together any odd layer j_1 from the first system and odd layer j_2 of second.

First Code \mathcal{G}_1

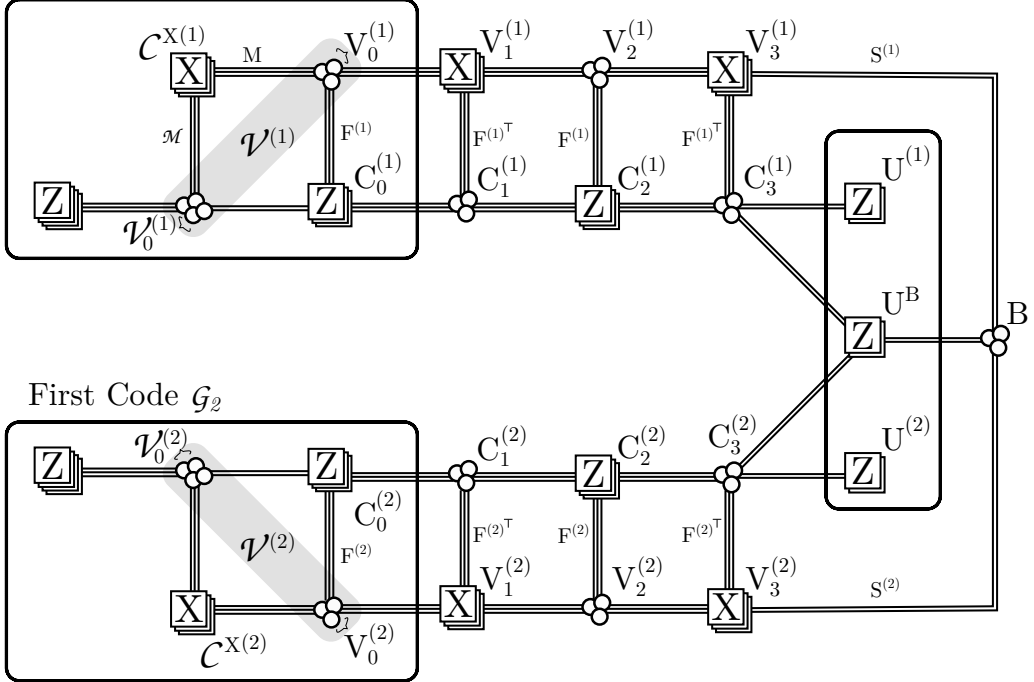


Figure 6: Redrawing the XX -system from Figure 5 in the special case that \bar{X}_1 and \bar{X}_2 come from separate code blocks.

A gauge check $Z(v_1 \in C_{j_1}^{(1)})Z(v_2 \in C_{j_2}^{(2)})Z(v_B \in B)$ in $U^{(1)}$, $U^{(2)}$, or U^B is a solution to

$$G \begin{pmatrix} v_1 & v_2 & v_B \end{pmatrix}^\top = 0. \quad (27)$$

Gauge checks in $U^{(1)}$ are solutions for which $v_2 = v_B = 0$ and checks in $U^{(2)}$ are solutions for which $v_1 = v_B = 0$. Clearly, $U^{(1)}$ and $U^{(2)}$ provide a basis for all solutions with $v_B = 0$.

If $v_B \neq 0$, we claim it has even weight if and only if v_1, v_2 exist so that (v_1, v_2, v_B) solves Eq. (27). This is because, for all v_1 , $Z(v_1 \in C_{j_1}^{(1)})$ must flip an even number of checks in $V_{j_1}^{(1)}$ (Lemma 8), or, equivalently $F^{(1)\top} v_1$ is even weight. Likewise, $F^{(2)\top} v_2$ is even weight. Therefore, (v_1, v_2, v_B) is a solution if and only if $S^{(1)} v_B$ and $S^{(2)} v_B$ are even weight, which implies v_B is even weight since $S^{(1)}$ and $S^{(2)}$ both have exactly one 1 per column.

As a result, we can choose a basis of U^B to consist of solutions in which $v_B = \hat{e}_i + \hat{e}_{i+1}$, for $i = 0, 1, \dots, |B| - 2$, where \hat{e}_i is the unit vector with a 1 in only the i^{th} position. \square

With the help of this lemma, we can show that the merged code indeed has $k - 1$ logical qubits.

Lemma 14. *The merged code \mathcal{G}_{XX} for measuring the product of two logical X operators has $k - 1$ logical qubits.*

Proof. First, notice that the original code \mathcal{G} with ancilla systems for measuring \bar{X}_1 and \bar{X}_2 would encode $k - 2$ logical qubits by applying Theorem 1 twice. Since \mathcal{G}_{XX} adds $|B|$ qubits and $|B| - 1$ independent checks (see Lemma 13) to that code, it encodes $k - 1$ logical qubits. \square

In practice, the joint measurement can be carried out with a schedule similar to the X measurement, Section 3.2 – starting from the original code, measure the stabilizers of the joint merged code for R rounds, and finally measure the stabilizers of the original code again. The qubits in V_i for even $i \geq 2$, C_j for $j \geq 1$ odd, and in B can be initialized in $|0\rangle$ at the zeroth round and measured out in the Z basis at the final round. Note this dispenses with the idea of preparing the module in a stabilizer state before the protocol

and preserving it in that state after the protocol in favor of simpler single-qubit preparations and final measurements. However, we can reach the same conclusions below if the modules for measuring \bar{X}_1 and \bar{X}_2 were kept intact as well.

In general, it would be nice if given individual ancilla systems for measuring \bar{X}_1 and \bar{X}_2 with only the guarantee that they have fault distance at least d , they can be connected via a bridge to measure $\bar{X}_1\bar{X}_2$ with fault distance at least d . Here \bar{X}_1 and \bar{X}_2 could be in the same codeblock or different codeblocks. Unfortunately, if they are in the same codeblock, there may exist another logical \bar{X}_3 (inequivalent to \bar{X}_1 , \bar{X}_2 , and $\bar{X}_1\bar{X}_2$) with weight larger than d whose weight is reduced to exactly d by both the \bar{X}_1 and \bar{X}_2 systems individually. In that case, the joint system could reduce the weight of \bar{X}_3 to below d by simply multiplying by the same checks from the individual systems that reduced the weight of \bar{X}_3 , provided there is sufficient cancellation of support on the bridge. Thus, the merged code \mathcal{G}_{XX} does not necessarily have good code distance. This suggests we can only prove something very general (without assuming more structure or expansion in the Tanner graph) in the case in which \bar{X}_1 and \bar{X}_2 are in separate codeblocks.

Another problem is that in the merged code for measuring $\bar{X}_1\bar{X}_2$, both \bar{X}_1 and \bar{X}_2 are still logical operators. However, it is not possible to use only the good fault distance properties of the individual ancilla systems to show the weights of \bar{X}_1 and \bar{X}_2 cannot be reduced since they are stabilizers in their respective individual systems.

We prove the following theorem about the fault distances of the joint ancilla system with a combination of assumptions we feel are reasonable. There are probably other sets of assumptions, perhaps including expansion, that could be turned into similar theorems. In specific and sufficiently small cases, it is possible to just compute the distances of the joint system, as we do in Section 4.

Theorem 15. *Suppose we begin with two separate codeblocks \mathcal{G}_1 and \mathcal{G}_2 and choose logical operators \bar{X}_1 and \bar{X}_2 , respectively, from those codes such that the X -ancilla systems for measuring them have measurement and logical fault distances at least d , and both \bar{X}_1 and \bar{X}_2 are minimal weight representatives of their logical equivalence classes. If we measure the merged code for $R \geq d$ rounds, then the joint measurement system connecting those ancilla systems via a bridge (see Figure 6) has measurement and logical fault distances at least d .*

Proof. Let \mathcal{S} be the stabilizer group of the original codes and each ancilla qubit, including bridge qubits, in $|0\rangle$, and \mathcal{S}_{XX} be the stabilizer group of the joint merged code, Figure 6. Also let \mathcal{L} be the group of logical operators of the unmeasured $k-1$ qubit logical space and $\mathcal{L}^* = \mathcal{L} \setminus \{I\}$. The versions of Lemmas 9 and 10 that apply to the joint code imply that the measurement fault distance is $\min(R, d_Z(\bar{Z}_1\mathcal{L}\mathcal{S}))$ and the logical fault distance is $\min(d_Z(\mathcal{L}^*\mathcal{S}), d_X(\mathcal{L}^*\mathcal{S}_{XX}))$. The original code \mathcal{S} has code distance at least d – if it did not, then the individual systems would not have fault distances at least d – and so $d_Z(\bar{Z}_1\mathcal{L}\mathcal{S}) \geq d$ and $d_Z(\mathcal{L}^*\mathcal{S}) \geq d$. To complete the proof, it remains only to show that the X -distance of the joint merged code is good, i.e. $d_X(\mathcal{L}^*\mathcal{S}_{XX}) \geq d$.

Suppose we have a logical X operator P from the merged code with stabilizer group \mathcal{S}_{XX} . We aim to show P is either trivial or has weight at least d .

Let Q_1 (resp. Q_2) denote all qubits of the merged code for measuring \bar{X}_1 out of \mathcal{G}_1 (resp. measuring \bar{X}_2 out of \mathcal{G}_2). Then, it is not hard to see $P_1 = P|_{Q_1}$ and $P_2 = P|_{Q_2}$ are logical operators (possibly trivial) of their respective merged codes. This is because they commute with all the checks of those codes.

If either P_1 or P_2 are nontrivial in their respective merged codes, then, by assumption, their weight and thus the weight of P is at least d . So assume both P_1 and P_2 are trivial.

This implies we can find $P' \equiv_{\mathcal{S}_{XX}} P$ such that P' is supported only on the bridge qubits B . Since P' must also commute with all checks in U^B and they have the structure of a repetition code on B (Lemma 13) this implies $P' = X(B)$ or I . Obviously, the latter case implies P is a stabilizer of \mathcal{S}_{XX} , so we proceed with the case $P' = X(B)$. Notice that $|P'| = |B| = \min(|\bar{X}_1|, |\bar{X}_2|) \geq d$. If we can show that the weight of $X(B)$ cannot be reduced by stabilizers, then also the weight of P is at least $|B| \geq d$.

Let S_1 be a product of X checks from the top half of Figure 6. That is, from the sets of checks $\mathcal{C}^{X(1)}$ and $V_j^{(1)}$ for odd j . We may write $S_1 = X(b_1 \in B)X(e_1)$ where e_1 is supported only on qubits in $\mathcal{V}_0^{(1)}$, $\mathcal{V}_i^{(1)}$ for

even i , and $C_j^{(1)}$ for odd j . Likewise, define $S_2 = X(b_2 \in B)X(e_2)$ as a product of checks from the bottom half of Figure 6.

This means that if $P'' = S_1S_2X(B)$ were to have less weight than $X(B)$, then $|e_1| + |e_2| = |e_1 + e_2| < |b_1 + b_2| \leq |b_1| + |b_2|$, where we used the fact that e_1 and e_2 have disjoint support for the first equality. In particular, it would have to be that either $|b_1| > |e_1|$ or $|b_2| > |e_2|$. Therefore, to show $|P''| \geq |B|$, it suffices to show that neither $S_1X(B)$ nor $S_2X(B)$ has less weight than $|B|$ for all possible choices of S_1 and S_2 .

These are similar arguments so we just provide a proof that $|S_1X(B)| \geq |B| \geq d$. Although $X(B) \equiv_{S_{XX}} \bar{X}_1$, the fact that the \bar{X}_1 system has code distance at least d is insufficient because \bar{X}_1 is actually a stabilizer in the merged code that measures it. Instead, let

$$S_1 = H_X(r \in \mathcal{C}^{X(1)}) \prod_{\substack{j=1 \\ j \text{ odd}}}^L H_X(v_j \in V_j^{(1)}), \quad (28)$$

for arbitrary choices of r and v_j . Splitting the X -check matrix of \mathcal{G}_1 into $M : \mathcal{C}^{X(1)} \rightarrow_X V_0^{(1)}$ and $\mathcal{M} : \mathcal{C}^{X(1)} \rightarrow_X \mathcal{V}_0^{(1)}$, we can calculate

$$X(B)S_1 = X(\vec{1} + v_L S^{(1)} \in B) \left(\prod_{\substack{i=2 \\ i \text{ even}}}^{L-1} X(v_{i+1} + v_{i-1} \in V_i^{(1)}) \right) X(v_1 + rM \in V_0^{(1)}) X(r\mathcal{M} \in \mathcal{V}_0^{(1)}) \quad (29)$$

$$\times \left(\prod_{\substack{j=1 \\ j \text{ odd}}}^L X(v_j F^{(1)\top} \in C_j^{(1)}) \right). \quad (30)$$

Since $|X(B)S_1|$ is at least the weight of factors in line 29, we proceed by ignoring the factors in line 30.

We note that $|X(\vec{1} + v_L S^{(1)} \in B)| = |\vec{1} + v_L S^{(1)}| \geq |B| - |v_L|$. Using this and the triangle inequality repeatedly, we find that $|X(B)S_1| \geq |B| - |v_L| + |v_L + rM| + |r\mathcal{M}|$. Applying the triangle inequality again, $|X(B)S_1| \geq |B| - |rM| + |r\mathcal{M}|$. Since \bar{X}_1 is minimal weight in its equivalence class, it must be that $|rM| \leq |r\mathcal{M}|$ for all r , which means $|X(B)S_1| \geq |B| = |X(B)|$ for all S_1 . \square

3.6 Gauged Y Ancilla System

Given the X and Z logical measurement schemes, in this section we present a Y measurement scheme that combines the two. Our proposal differs from the one presented in [CKBB22] because that proposal relies on using $2d - 1$ layers to achieve fault-distance d .

Again we make use of a bridge system like in the joint measurement case of the previous section. Here, however, we use the bridge to connect the X and Z systems together on the first layer, where they are also joined by a mixed-type check q_1 . See Figure 7 for the full construction.

For convenience in this section, we make the assumption that \bar{X}_M and \bar{Z}_M overlap on exactly one qubit. This makes the structure of gauge checks in the Y -system easier to reason about in proofs. However, we do not believe this is necessary and that all arguments in this section should generalize to cases of larger overlap (see also Remark 17 below).

Lemma 16. *A complete, linearly independent basis for the gauge checks in U^B in the Y system consists of $|B|$ checks. Moreover, there is a choice of basis in which there is exactly one check acting on each bridge qubit in B .*

Proof. We describe connectivity between checks q_1, V_1^Z, V_1^X and qubits C_1^X, C_1^Z, B by defining a matrix with rows corresponding to those checks and column corresponding to those qubits. Looking at Figure 7, this is

$$G = \begin{pmatrix} f^{Z\top} & f^{X\top} & 0 \\ F^{Z\top} & 0 & S^Z \\ 0 & F^{X\top} & S^X \end{pmatrix}. \quad (31)$$

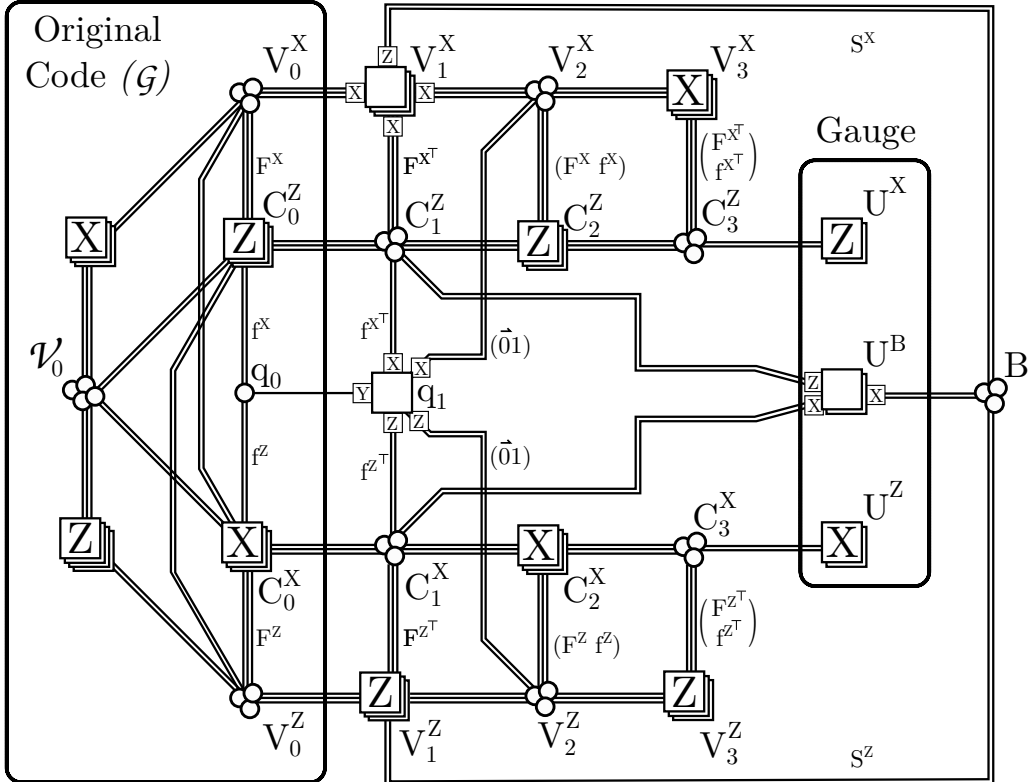


Figure 7: The ancilla system for measuring \bar{Y} where \bar{X} and \bar{Z} overlap on one qubit q_0 . It largely consists of the ancilla systems for measuring \bar{X} and \bar{Z} separately, but with changes to the first layer, and the addition of the bridge qubits B and more gauge checks U^B . The first layer introduces just one check q_1 connected to q_0 and has sets of checks V_1^X and V_1^Z which are each one smaller than sets in higher layers, e.g. V_3^X and V_3^Z .

Let v_X indicate a subset of C_1^X qubits, v_Z a subset of C_1^Z , and v_B a subset of B . Gauge check $X(v_X \in C_1^X)Z(v_Z \in C_1^Z)X(v_B \in B)$ is defined as a solution to

$$G \begin{pmatrix} v_X & v_Z & v_B \end{pmatrix}^\top = 0. \quad (32)$$

In particular, gauge checks in U^X are solutions for which $v_Z = v_B = 0$ and gauge checks in U^Z are solutions for which $v_X = v_B = 0$.

We claim that solutions $(v_X, v_Z, 0)$ with $v_B = 0$ are the sum of solutions in U^X and U^Z . Note that, for any v_X , applying $X(v_X \in C_1^X)$ flips an even number of checks from $V_1^Z \cup q_1$ (see Lemma 8). Therefore, because $F^{Z^\top} v_X^\top = 0$, meaning v_X flips no checks in V_1^Z , v_X also does not flip q_1 or $f^{Z^\top} v_X^\top = 0$. This shows $(v_X, 0, 0)$ is a solution to Eq. (32). Likewise, it can be argued $(0, v_Z, 0)$ is a solution.

Therefore, beyond those corresponding to gauge checks in U^X and U^Z , the only other independent solutions are those with $v_B \neq 0$. In fact, for all $v_B \neq 0$, there exist v_X and v_Z such that (v_X, v_Z, v_B) solves Eq. (32). We show this for a basis $v_B = \hat{e}_i$, the unit vector with a 1 in only the i^{th} position.

The i^{th} bridge qubit is connected to two checks, one i_X in V_1^X and one i_Z in V_1^Z . This is equivalent to saying $S^X \hat{e}_i^\top = \hat{e}_{i_X}^\top$ and $S^Z \hat{e}_i^\top = \hat{e}_{i_Z}^\top$.

Using Lemma 8, we can find a vector v_X such that $f^{Z^\top} v_X^\top = 1$ and $F^{Z^\top} v_X^\top = \hat{e}_{i_X}^\top$ because $X(v_X \in C_1^X)$ flips exactly two checks, i_X and q_1 . Likewise, we find v_Z such that $f^{X^\top} v_Z^\top = 1$ and $F^{X^\top} v_Z^\top = \hat{e}_{i_Z}^\top$. It is then easy to verify that (v_X, v_Z, v_B) solves Eq. (32). \square

Remark 17. It is important to note that if \bar{X}_M and \bar{Z}_M overlap on more than one qubit, the above proof may no longer hold, and the Y merged code may have extra gauge qubits. These gauge checks take the form of $X(u \in C_1^X)Z(v \in C_1^Z)$, where u and v are chosen to ensure commutation with checks in V_1^X , V_1^Z , and the new collection of checks Q_1 , $|Q_1| > 1$, which replaces q_1 . In particular, $Z(v \in C_1^Z)$ flips an even number of checks in $V_1^X \cup Q_1$ and $X(u \in C_1^X)$ flips an even number of checks in $V_1^Z \cup Q_1$. If the only checks they flip are both the same set of checks from Q_1 , then $X(u \in C_1^X)Z(v \in C_1^Z)$ is a gauge operator. This also explains why there are no gauge checks of this form if $Q_1 = \{q_1\}$, because it is impossible to flip an even number of checks from a set of size one. In general, these gauge checks should be fixed as well to ensure the system encodes just $k - 1$ qubits.

Knowing the structure of the gauge checks allows us to prove that the Y system encodes exactly $k - 1$ qubits, though we defer the proof to Appendix A.2.

Theorem 18. *The Y -system encodes $k - 1$ qubits.*

Ideally, one would also be able to show that the Y -system has good fault-distance if the individual X and Z systems do. However, the proof of fault-distance is complicated by the non-CSS nature of the merged code, meaning we lack a lemma similar to Lemma 10. In specific cases, one can check the fault distance by applying Lemma 9 with $\mathcal{U} = \langle \mathcal{S}_O, \mathcal{S}_Y \rangle$ and $\mathcal{L} = \langle \bar{X}_i, \bar{Z}_i, i = 1, 2, \dots, k - 1 \rangle$, where \mathcal{S}_O is the stabilizer group of the original code (with the additional qubits starting in $|+\rangle$ for the bottom half of Figure 7 and the bridge and in $|0\rangle$ for the top half), \mathcal{S}_Y the stabilizer group of the merged code shown in Figure 7, and \mathcal{L} a simultaneous $k - 1$ qubit logical basis for each of the codes $\mathcal{S}'_O = \langle \mathcal{S}_O, \bar{Y}_M \rangle$, \mathcal{S}_Y and \mathcal{U} .

Without the bridge qubits, $\bar{Z}_M \mathcal{U}$ would clearly contain a low-weight element, namely $P = \bar{Z}_M q_1 \mathcal{H}_Z(V_{j \text{ odd}}^Z)$, where $\mathcal{H}_Z(V_{j \text{ odd}}^Z)$ is the product of all Z checks in the sets V_1, V_3, \dots . Notice that P would then have weight equal to the weight of the X -type part of q_1 , which is a constant-weight check. The presence of the bridge qubits is therefore essential to eliminating this and similar cases that lead to low measurement fault distance.

We can at least prove that the code distance of the merged code with stabilizer group \mathcal{S}_Y is good.

Theorem 19. *If the X -system and Z -system individually have code distances at least d , then the Y -system has code distance at least d .*

Proof. Suppose \bar{P} is a nontrivial logical operator of \mathcal{G}_Y , the merged code of the Y system. We aim to show that it has weight at least d . Let $\bar{P} = P_X P_Z$ be its decomposition into an X -type Pauli P_X and Z -type Pauli P_Z .

Throughout we let \mathcal{G}_X and \mathcal{G}_Z denote the merged codes of the X - and Z -systems, respectively. When we write $P'_X = P_X|_{\mathcal{G}_X}$ or $P'_Z = P_Z|_{\mathcal{G}_Z}$, we mean to restrict those operators originally supported on \mathcal{G}_Y to the qubits that exist in \mathcal{G}_X or \mathcal{G}_Z , respectively.

We note that P'_X is a logical operator on \mathcal{G}_X . It commutes with all Z checks of \mathcal{G}_X because \bar{P} commutes with all the checks of \mathcal{G}_Y . Similarly, P'_Z is a logical operator of \mathcal{G}_Z .

We next claim that either P'_X is a nontrivial logical operator of \mathcal{G}_X or P'_Z is a nontrivial logical operator of \mathcal{G}_Z . This can be seen by contradiction. Assuming both P'_X and P'_Z are products of stabilizers in their respective codes, then \bar{P} can also be multiplied by the respective stabilizers from \mathcal{G}_Y to find an equivalent operator with support that is much restricted:

$$\bar{P} \equiv_{\mathcal{S}_Y} Z(v_Z \in C_{j \text{ odd}}^Z \cup V_{i \text{ even}}^X) X(v_X \in C_{j \text{ odd}}^X \cup V_{i \text{ even}}^Z) Z(b_Z \in B) X(b_X \in B), \quad (33)$$

where we used $C_{j \text{ odd}}^Z$ to mean $\bigcup_{j \text{ odd}} C_j^Z$ and similarly for the other variants of this notation. Furthermore, by multiplying with gauge checks U^X, U^Z, U^B and checks from $C_{j \text{ odd}}^Z$ and $C_{i \text{ even}}^X$ we can move the support of $\bar{P} \equiv_{\mathcal{S}_Y} Z(b'_Z \in B) X(b'_X \in B)$ entirely onto the bridge qubits B (this goes like the proof of Theorem 3 so we omit the details). However, in order to commute with all checks in U^B (see Lemma 16), V_1^Z , and V_1^X , it must be that $b'_Z = b'_X = 0$ or $\bar{P} \equiv_{\mathcal{S}_Y} I$. This is impossible because then \bar{P} would be a nontrivial logical operator of \mathcal{G}_Y .

Now to conclude the proof, we simply note that P'_X being nontrivial in \mathcal{G}_X implies $|P'_X| \geq d$ by assumption. Since $|\bar{P}| \geq |P_X| \geq |P'_X| \geq d$, we obtain the desired lower bound on $|\bar{P}|$ in this case. Likewise, if P'_Z is nontrivial in \mathcal{G}_Z , we find $|\bar{P}| \geq |P_Z| \geq |P'_Z| \geq d$. \square

4 Case Study: Gross Code

In this section we apply the techniques from the prior section to construct an ancilla system tailored for the $[[144, 12, 12]]$ code presented by [BCG⁺24], known as the gross code. We present an ancilla system with an additional 103 physical qubits, 54 data and 49 check, that are capable of implementing various logical measurements. Together with the automorphism gates that are readily implementable in the gross code, these measurements enable synthesis of all logical Clifford gates and all logical Pauli measurements of eleven of the twelve logical qubits in the code. Prior work in [BCG⁺24] gave an ancilla system that requires 1380 additional qubits and is merely capable of logical data transfer into and out of the code.

We begin with a review of the construction of the gross code, and Bivariate Bicycle codes more generally. The Tanner graph of the code features vertices of four types: X and Z check vertices, and L and R data vertices. For some $l, m \in \mathbb{Z}^+$, there are lm vertices in each of these categories. The vertices are labeled by elements of an abelian group $\mathcal{M} := \langle x, y | x^l, y^m \rangle \cong \mathbb{Z}_l \times \mathbb{Z}_m$ which can be viewed as gridpoints on a $l \times m$ torus. Elements of the X set can be written as $X(x^i y^j)$ for some $0 \leq i < l$ and $0 \leq j < m$, and similarly for the Z, L , and R sets. This makes for $2lm$ check qubits and $2nm$ data qubits. For the gross code, $l = 12$ and $m = 6$.

The edges of the Tanner graph are specified by two polynomials $A, B \in \mathbb{F}_2[\mathcal{M}]$ with three terms each. For example, for the gross code we have:

$$A := x^3 + y + y^2, \quad B = y^3 + x + x^2. \quad (34)$$

Since the polynomials are over \mathbb{F}_2 , they are also naturally interpreted as subsets of \mathcal{M} . Then the Tanner graph is given as follows. For some $m \in \mathcal{M}$, the vertex $X(m)$ is connected to the vertices $L(Am) := \{L(m') \text{ for } m' \text{ in } Am\}$, and to $R(Bm) := \{R(m'') \text{ for } m'' \text{ in } Bm\}$. Similarly, if A^\top is the polynomial consisting of the inverses of the monomials of A , that is, $A^\top = x^{-3} + y^{-1} + y^{-2}$, then the vertex $Z(m)$ is connected to $L(B^\top m) := \{L(m') \text{ for } m' \text{ in } B^\top m\}$, and to $R(A^\top m) := \{R(m'') \text{ for } m'' \text{ in } A^\top m\}$.

We verify that the checks commute. Lemma 2 of [BCG⁺24] shows that an X operator on $L(p) \cup R(q)$ anticommutes with a Z operator on $L(\bar{p}) \cup R(\bar{q})$ if and only if $p\bar{p}^\top + q\bar{q}^\top$ contains the monomial $1 \in \mathcal{M}$. The $X(m)$ check is supported on $L(Am) \cup R(Bm)$, and the $Z(m')$ check is supported on $L(B^\top m') \cup R(A^\top m')$.

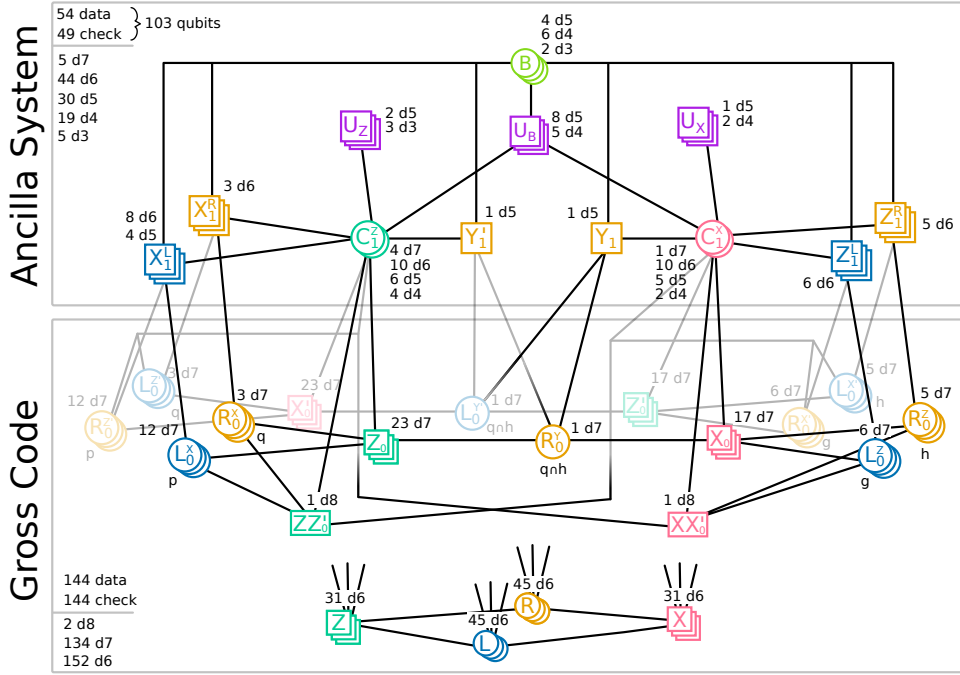


Figure 8: Qubit and degree counts of a gross code equipped with an ancilla system. This ancilla system implements eight different logical measurements by realising different subgraphs as Tanner graphs. Circular qubits are data, and squares are checks. Gauge checks are in purple, the bridge is green, and the remaining ancilla system qubits are colored according to their partners in the gross code: X is red, Z is teal, R is oRange, and L is bLue. The ancilla system is connected to two pairs of logical operators that are ZX -duals of one another: the \bar{X}, \bar{Z} qubits are opaque and the \bar{X}', \bar{Z}' qubits are transparent. Their Tanner-subgraphs overlap on the ZZ'_0 and XX'_0 qubits. Note that checks are labeled X or Z type according to how they are used in X or Z systems individually, but in the joint measurement and Y systems that employ the bridge, they are no longer mono-type checks (see Figs. 5 and 7). An annotation ‘3 d7’ means that there are three degree-seven qubits.

We observe that $(Am)(B^\top m')^\top + (Bm)(A^\top m')^\top = m(m')^\top(AB + AB) = 0$ which never contains 1, so the stabilizers must always commute.

Logical Pauli operators on the gross code feature two symmetries of the type studied by [BB24]: automorphisms and a ZX -duality. Automorphisms correspond to shifts of a logical operator by a monomial $w \in \mathcal{M}$. Suppose a logical X operator supported on $L(p) \cup R(q)$ commutes with all Z stabilizers, and hence obeys $pB + qA = 0$. Then we have $(wp)B + (wq)A = 0$ for all $w \in \mathcal{M}$, so $L(wp) \cup R(wq)$ is also the support of a logical X operator. The same argument holds for Z operators. The permutation of the physical qubits corresponding to multiplying by a monomial has a fault tolerant quantum circuit.

The ZX -duality is a permutation that converts the support of an X check to that of a Z check, and vice versa. Again, if a logical X operator is supported on $L(p) \cup R(q)$, then $pB + qA = 0$. This implies $B^\top p^\top + A^\top q^\top = 0$, so a Z operator supported on $L(q^\top) \cup R(p^\top)$ commutes with the X stabilizer. [BCG⁺24] constructed a high-depth fault-tolerant circuit implementing this permutation, but this scheme does not seem practical. Nonetheless we find the ZX -duality useful in the construction of our ancilla system.

For every qubit defined by an anticommuting \bar{X}, \bar{Z} pair, there exists a ‘primed’ qubit defined by applying the ZX -duality to these operators, obtaining \bar{Z}', \bar{X}' . Hence, the twelve logical qubits of the gross code decompose into a primed and unprimed block, each with six logical qubits, on which the automorphism gates act simultaneously and identically.

Having reviewed the gross code, we proceed with the description of the ancilla system.

4.1 Mono-layer ancilla system

A sketch of the system is shown in Figure 8, displaying an overview of the layout of the ancilla system as well as its resource requirements. The construction is based on a pair of logical X and Z operators where a mono-layer measurement scheme preserves code distance. In particular, we have an \bar{X} operator supported on $L(p) \cup R(q)$, and a \bar{Z} operator supported on $L(r) \cup R(s)$ where:

$$p = y + xy^5 + x^2y^2 + x^2y^4 + x^3y + x^3y^2 + x^4y + x^4y^2 + x^9y^3 + x^{10} + x^{11} + x^{11}y^3, \quad (35)$$

$$q = y^2 + xy + xy^5 + x^6, \quad (36)$$

$$r = x^2y^3 + x^2y^5 + x^3 + x^3y^3 + x^3y^4 + x^3y^5, \quad (37)$$

$$s = xy^3 + xy^5 + x^2 + x^2y^4 + x^3y^2 + x^3y^4. \quad (38)$$

We verify numerically using CPLEX that the distance of the merged codes of the X and Z systems individually are both 12, preserving the distance of the original code. These operators overlap only on $R(xy^5)$, so they anticommute.

Several additional ancilla systems can be constructed from these X and Z systems. We present a single graph of connected qubits, such that a supercomputing architecture based on this graph can realize all of these systems either with a direct correspondence of qubits to Tanner graph vertices, or with a few flag qubits for $R(xy^5)$ only.

- Following the construction in section 3.6, we can build a system that measures $\bar{Y} := i\bar{X}\bar{Z}$. This introduces eleven bridge qubits that connect the two ancilla systems - one fewer than the distance since they already share $R(xy^5)$. These are shown in Figure 9. In the resulting Tanner graph there is one qubit in the ancilla system connected to $R(xy^5)$ that connects the X and Z systems together. For reasons we explain shortly, we will split this vertex into three logical qubits connected in a line. These three qubits can act as a single check by initializing all but the middle qubit in a Bell state, and finishing with a Bell measurement. This yields a few flag measurements [DA07].
- Due to the ZX -duality, the operator \bar{Z} has a dual X logical operator supported on $L(s^\top) \cup R(r^\top)$. To arrive at disjoint operators and also to minimize overlap of check qubits, we subsequently apply an automorphism $w = x^{10}y^5$, and arrive at an operator \bar{X}' supported on $L(ws^\top) \cup R(wr^\top)$. Similarly, we construct an operator \bar{Z}' supported on $L(wq^\top) \cup R(wp^\top)$. Since \bar{X}' was constructed from \bar{Z} using geometric symmetries of the code, the subgraph of the Tanner graph used to construct the ancilla system is identical for these operators up to a switch of X and Z . By connecting the \bar{Z} ancilla system to both of the \bar{Z} and \bar{X}' subgraphs, a single system can measure both \bar{Z} and \bar{X}' by considering different subsets of the connections as the Tanner graph. Similarly, the \bar{X} system can also measure \bar{Z}' . We can also measure $\bar{Y}' := i\bar{X}'\bar{Z}'$.
- Following section 3.5, we construct measurements of the joint operators $\bar{X}\bar{X}'$ and $\bar{Z}\bar{Z}'$. This explains the need to split the $R(xy^5)$ qubit: since \bar{X} and \bar{X}' are disjoint, the ancilla qubits connected to $R(xy^5)$ and its dual $L(w(xy^5)^\top)$ need to be separate. Now, twelve bridge qubits are required to ensure preservation of code distance. As anticipated above, we place this bridge qubit between the two qubits connected to $R(xy^5)$, so that these qubits can act as a single check together when we are measuring \bar{Y} or \bar{Y}' .

Hence the same ancilla system can measure any of the operators $\bar{X}, \bar{Y}, \bar{Z}, \bar{X}', \bar{Y}', \bar{Z}', \bar{X}\bar{X}',$ and $\bar{Z}\bar{Z}'$. In section 4.3 we show that these measurements and the automorphisms together can synthesize all Clifford gates on eleven of the twelve qubits.

The theorems proved in Section 3 generally do not provide enough evidence to conclude that the $\bar{Y}, \bar{Y}', \bar{X}\bar{X}',$ and $\bar{Z}\bar{Z}'$ merged codes preserve code distance. Nevertheless we find numerically that this is the case using CPLEX.

In the original gross code all vertices in the Tanner graph have degree six. Looking at Figure 8, the degrees of the qubits in the ancilla system are mostly equal or less than this since the subgraphs of the

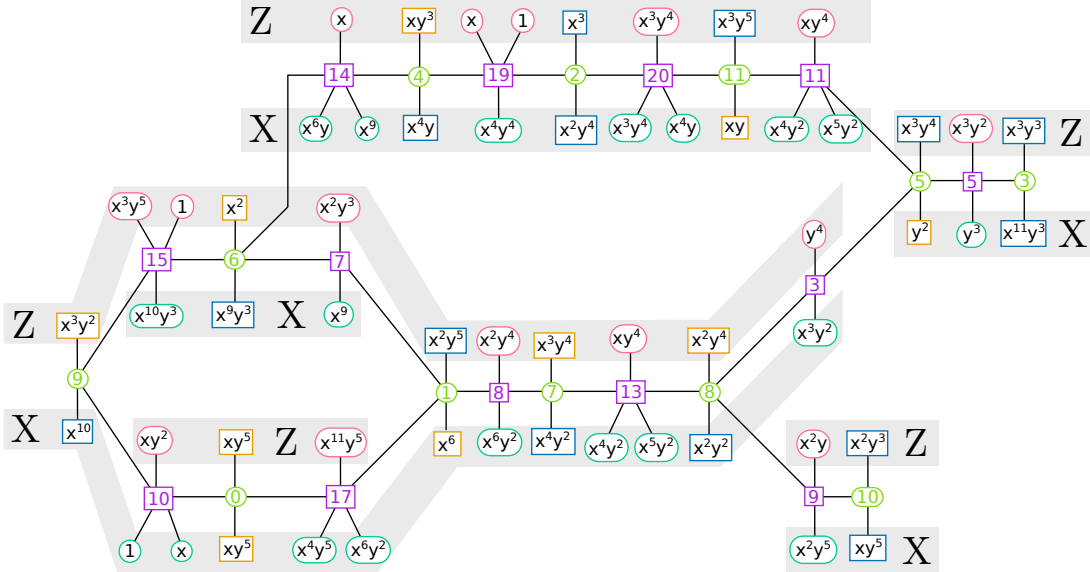


Figure 9: Subgraph of the Tanner graph corresponding to the bridge and its corresponding gauge checks. The bridge system is necessary to ensure that $\bar{X}\bar{X}'$, $\bar{Z}\bar{Z}'$, \bar{Y} , and \bar{Y}' measurements are fault tolerant. Each green bridge qubit connects a pair of checks in the X and Z systems. This introduces several loops, which give rise to gauge degrees of freedom, which are removed through additional checks in purple.

gross code corresponding to the logical operators do not include connections to one type of check. However, the additional gauge checks introduced by the bridge system result in some degree seven data qubits in the ancilla. Many qubits in the gross code must be connected to the ancilla system. Through careful choice of the automorphism shift w , it was achieved that all but two of these qubits connect to the ancilla system only once, so they have degree seven. The qubits $X(x^{11}x^5)$ and $Z(x^{11})$ are the only degree eight qubits in the construction. If it had not been split via the bridge, the shared $R(xy^5)$ qubit in the ancilla system would have had degree eight as well.

Several gauge checks were introduced, either supported in the X or Z systems alone, or to deal with loops introduced by the bridge. The gauge checks are specified in Figures 9 and 10. For the full $\bar{X}\bar{X}'$ and $\bar{Z}\bar{Z}'$ measurement operations all of these gauge checks are necessary. But for the other measurements, it turns out that several of the gauge checks are redundant. In the \bar{X} , and \bar{Z}' systems one *only* needs gauge checks 0, 1, and 2. In the \bar{Z} and \bar{X}' systems one only needs gauge check 6. In the \bar{Y} and \bar{Y}' systems, gauge checks 10 and 17 must have their support from bridge qubit 0 removed in order to be well-defined. Then, gauge checks 6, 12, 16, 17, 18, and 20 are redundant.

4.2 Numerical simulations

We perform circuit-level noise simulations of the measurement protocols for the X and Z ancilla systems. We find that the syndrome circuits for the corresponding merged codes preserve the circuit-level distance of the gross code's circuit, which is ten. Due to the larger circuit size, the resulting logical error rates per syndrome cycle are about a factor of ten larger than a syndrome cycle with no logical gate. These results suggest that measurements implemented via ancilla systems are a practical avenue for implementing fault-tolerant logical gates in an architecture based on the gross code.

The syndrome circuit is derived from an edge-coloring of the Tanner subgraph shown in Figure 10. The full circuit is shown in Figure 14. The coloring yields a quantum circuit with three rounds marked R , G , and B in the figure, and one additional ‘early’ round, that together cover all edges in the subgraph supported on the ancilla system. The syndrome circuit of the gross code has eight rounds of CNOTs or measurements and features a natural gap where the data qubits are idling. This gap is leveraged for implementing the edges between the ancilla system and the gross code, so the merged syndrome circuit has the same depth

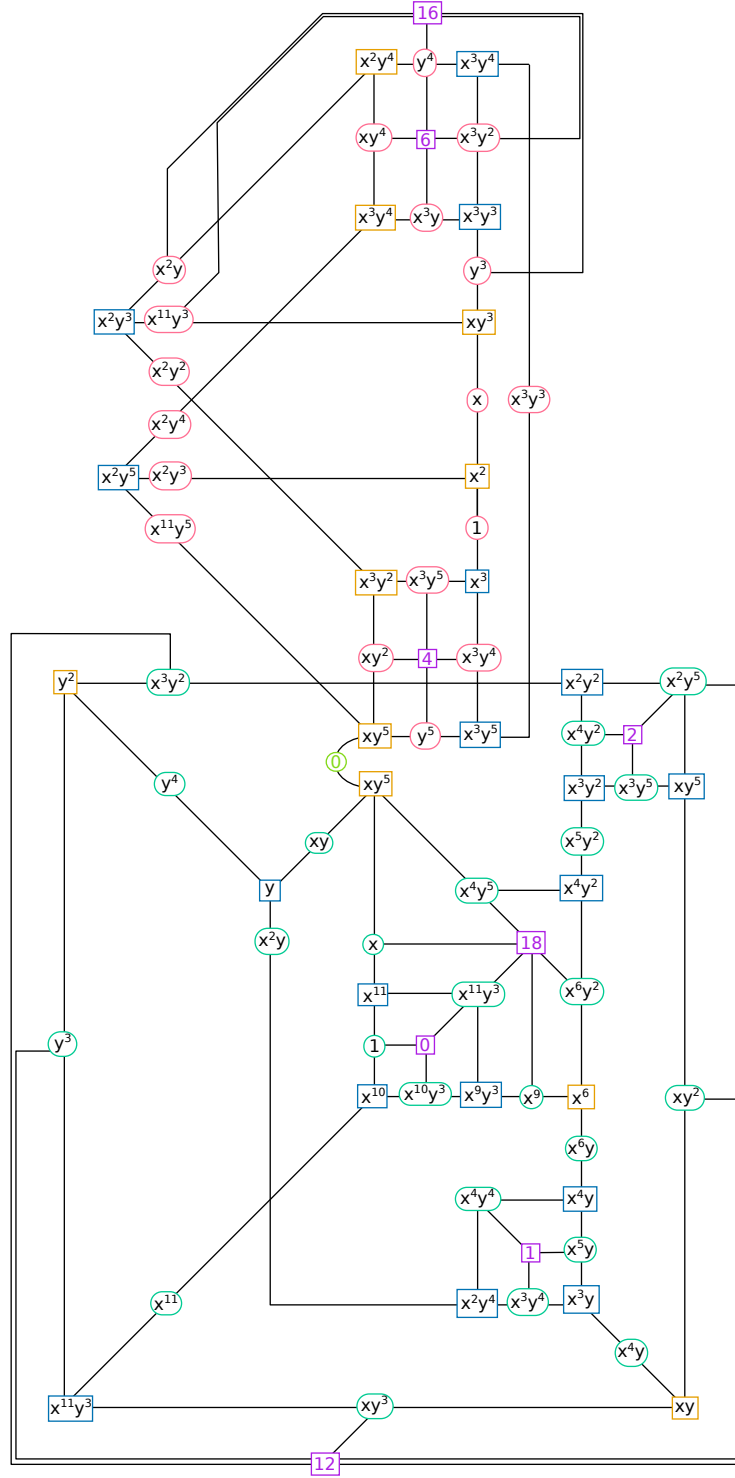


Figure 10: Subgraph of the Tanner graph of the ancilla system ignoring the bridge, except for bridge qubit 0 which connects the qubits corresponding to the $R(xy^5)$ where \bar{X} and \bar{Z} overlap. Qubits are labeled by the qubit they are connected to in the gross code, following the coloring scheme described in Figure 8. Observe how the role of check and data qubits are reversed relative to the gross code qubits.

per cycle.

Recall that for the X and Z systems, we can ignore the gauge checks 4, 12, and 18 since they are redundant, as well as the bridge qubit 0. Hence, the X and Z Tanner graphs in Figure 10 have vertices with degree at most three, except for the gauge check 6 which has degree four. We find that, if we leave out one of check 6's edges, the edges of the graph are three-colorable, yielding a depth-three quantum circuit that includes all required CNOT gates. If all the checks in the circuit were the same type of check (all X or all Z), then the order of these CNOTs would not matter. However, since gauge checks are of a different type, the original coloring circuit results in some incorrect computation of the stabilizers near the gauge checks. We find that this is easily fixed by introducing an additional 'early' round of CNOTs, and moving some of the problematic CNOTs into this round. This is also a natural spot for the fourth edge of the gauge check 6. See Figure 15 for a derivation and specification.

We perform three experiments on the syndrome circuits. First, we perform a memory experiment to empirically determine the circuit-level distance and to compare to the code's idle cycle. Second, we determine how many syndrome cycles are suitable for a logical measurement by comparing the logical error rate to the measurement error rate. Both of these experiments rely on the modular decoding approach described in Section 3.4. In the third experiment we assess the benefits of the modular decoding approach over a simpler implementation relying on BPOSD alone. Our software is implemented in python and leverages the `stim` [Gid21], `pymatching` [HG23], and `bp_osd` [RWBC20, Rof22] libraries.

The memory experiment is shown in Figure 11a). We compare the X and Z systems as well as the operation of the gross code syndrome cycle on its own. We find that our simulations of the gross code match the fits from [BCG⁺24] within statistical error, confirming the accuracy of our implementation and that our error model is the same as the one described in their Section 2. The logical error rates of the X and Z systems are within a factor of 10x and 5x larger than that of the code on its own. We also conclude that the circuit-level distance of all the syndrome circuits is ten, both from the similarity of the slopes of the curves, and also BPOSD's inability to identify undetectable logical errors of weight less than ten.

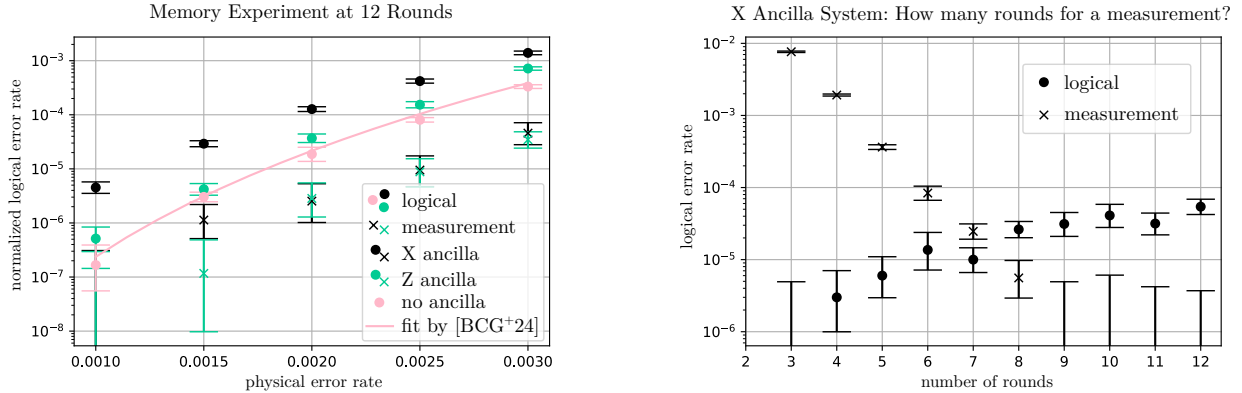
In Figure 11b) we compare the error rate of the logical measurement to the logical error rate - the probability of a logical error on any of the qubits not being measured. As the number of rounds increases there are more opportunities for high-weight errors and the logical error rate increases. But more rounds also provide more measurements of the stabilizers composing \bar{X} , yielding a more reliable logical measurement outcome. We find that these probabilities are about the same at seven rounds, although this crossover point will depend on the physical error rate. In this experiment the physical error rate was 0.001.

All experiments above rely on the modular decoding method from Section 3.4. In Figure 12 we compare this modular decoder to a purely BPOSD decoding approach in the critical region of about seven syndrome cycles at a physical error rate of 0.001. Here we find that the performance of the two decoders is very similar up to statistical error, with a slight advantage towards a purely BPOSD approach. However we also see that the matching decoder is over 100x faster than the BPOSD decoders, and the BPOSD decoder for the merged code is about 10x slower than that of the gross code alone. This shows that the modular decoding approach can provide a tangible improvement in decoding time.

4.3 Implementing logical Clifford gates

Together with the automorphisms the logical measurements implemented by the ancilla system suffice to implement all logical Clifford gates on eleven of the twelve logical qubits.

Automorphism gates are permutations of the physical qubits, and hence take X operators to X operators and Z operators to Z operators. Since \bar{X} is supported on $L(p) \cup R(q)$, we may define \bar{X}_α to be supported on $L(\alpha p) \cup R(\alpha q)$ for $\alpha \in \mathcal{M}$. A measurement of \bar{X}_α can be implemented by conjugating an \bar{X} measurement with the automorphism gate α . We further let \bar{Z}_α be supported on $L(\alpha s^\top) \cup R(\alpha r^\top)$, and similarly for the dual operators \bar{X}'_α and \bar{Z}'_α . For the joint measurements \bar{Y} , \bar{Y}' , $\bar{X}\bar{X}'$ and $\bar{Z}\bar{Z}'$ we cannot apply automorphisms to each operator in the product separately. We only have access to $\bar{Y}_\alpha := i\bar{X}_\alpha \bar{Z}_\alpha$, and $\bar{Y}'_\alpha := i\bar{X}'_\alpha \bar{Z}'_\alpha$, as well as $\bar{X}_\alpha \bar{X}'_\alpha$, and $\bar{Z}_\alpha \bar{Z}'_\alpha$. Note that there is a set of α such that $\bar{X}_\alpha, \bar{Z}_\alpha, \bar{X}'_\alpha, \bar{Z}'_\alpha$ form a symplectic basis for the logical Hilbert space. For such a basis can individually initialize and read all logical qubits.



a) Comparison of logical error rates of the X and Z ancilla systems and the idle gross code in the circuit-level noise model for 12 syndrome cycles. Logical error rates are normalized by the number of syndrome rounds. A logical error is any error on the logical qubits not being measured.

b) Comparison of the logical measurement error to the probability of a logical error on the remaining qubits. Here we consider the X system at a physical error rate of $p = 0.001$. At this physical error rate the quantities are balanced at about seven rounds.

Figure 11: Circuit-level noise model benchmarks of the merged syndrome circuits shown in Figure 14. The noise model is the same as that of [BCG⁺24]. The error bars denote confidence intervals of 1σ .

To transform our measurement-based gateset into a unitary gate set, we make use of the following well-known identity (e.g., [Lit19] Figure 11b).

$$\begin{array}{c} \text{Circuit Diagram:} \\ \text{Left: } |0\rangle \xrightarrow{\text{X}} \text{Box P} \xrightarrow{\text{Y}} \text{Box P}^a \xrightarrow{\text{X}} \text{Box P}^{a+b+1} \xrightarrow{\text{Y}} \text{Box P}^b \xrightarrow{\text{a}} |0\rangle \\ \text{Right: } |0\rangle \xrightarrow{\text{e}^{i\frac{\pi}{4}P}} |0\rangle \end{array} = \quad (39)$$

Here P is any n -qubit Pauli matrix, and for our purposes we are interested in $n = 11$. A Clifford gate of the form $e^{i\frac{\pi}{4}P}$ is called a Pauli rotation.

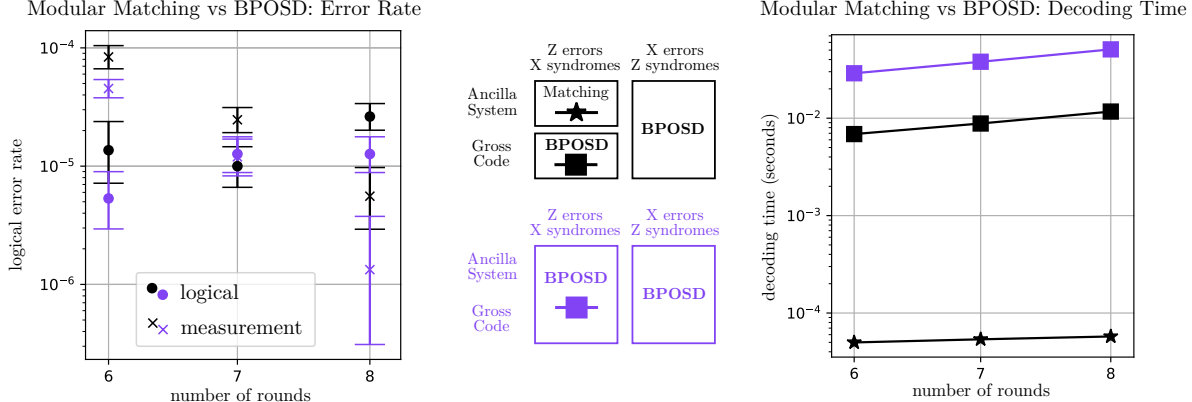
Any measurement-based unitary synthesis strategy must sacrifice one qubit to act as a ‘pivot’ - here the bottom qubit in the circuit. The pivot ensures that the measurement outcome is never deterministic, and hence cannot decohere the quantum information on the data qubits. Measurement-based operations repeatedly entangle and disentangle the data qubits with the pivot qubit. The measurement results generate Pauli corrections which are cheap to apply, either physically or by tracking the Pauli frame.

There are some variations of (39). The $|0\rangle$ initialization can be performed through a Z measurement, resulting in a $Z \rightarrow X \rightarrow Y$ sequence of basis changes. By inserting single-qubit Clifford gates and their inverses, this sequence can be changed to any ordering of the X, Y, Z bases.

We select the pivot qubit to be the logical qubit with operators \bar{X}_1 and \bar{Z}_1 . This way we can implement measurements of \bar{X}_1 , \bar{Z}_1 , and \bar{Y}_1 natively using the ancilla system. Hence, *any* implementable measurement can be transformed into a Pauli rotation so long as it has support on both the pivot qubit and at least one other logical qubit. No matter if the support on the pivot is X , Y , or Z , we can select the initialization and final measurement in (39) to be the other two.

The automorphism group is given by \mathcal{M} , with $|\mathcal{M}| = 72$. However, we find that logical operators are invariant under the automorphism x^6 : $\bar{X}_1\bar{X}_{x^6}$ and $\bar{Z}_1\bar{Z}_{x^6}$ are in the stabilizer. Hence if we consider the group of automorphism unitaries modulo the stabilizer, this group has order 36.

With 36 (logical) automorphisms and eight logical Pauli measurements from the ancilla system, we can implement 288 logical measurements. But any conjugated measurement of $\bar{X}', \bar{Y}', \bar{Z}'$ would have support on the primed qubits only, and hence cannot have support on the pivot since it is in the unprimed block. Therefore, only $(8 - 3) \times 36 = 180$ measurements are useful for rotation synthesis. Of these, 95 have support on both the pivot and the remaining qubits.



a) Measurement and logical error rates of two different decoding strategies. We see that these are very similar up to statistical error, with a purely BPOSD strategy performing slightly better.

b) Decoding compute times for the decoding strategies, leveraging the `bp.osd` and `pymatching` python packages. We see a significant improvement for the modular approach.

Figure 12: Comparison of the modular decoding strategy to a decoder based purely on BPOSD. Here we consider the X ancilla system, a number of cycles where measurement and logical errors are similar, and a physical error rate $p = 0.001$. The error bars denote confidence intervals of 1σ .

We find that these 95 rotations suffice to generate the Clifford group. This is verified numerically via brute-force search. We leverage the following identity:

$$e^{i\frac{\pi}{4}P} e^{i\frac{\pi}{4}Q} e^{-i\frac{\pi}{4}P} = \begin{cases} e^{\frac{\pi}{4}PQ} & \text{if } PQ = -QP \\ e^{i\frac{\pi}{4}P} & \text{otherwise} \end{cases}, \quad (40)$$

noting that $e^{\frac{\pi}{4}PQ}$ is unitary since PQ is anti-Hermitian. We maintain a list of implementable Pauli rotations, and grow this list by conjugating them by rotations from the 95 natively implementable gates. When a new implementable rotation is found it is added to the list. When a shorter implementation of a prior rotation is found the recorded implementation is updated with the shorter one. We terminate the search when all implementations are found. Since the Clifford group is generated by Pauli rotations and Pauli matrices [Cal76] this suffices to show that all Clifford gates can be implemented.

The search algorithm above finds partially optimized but not necessarily optimal implementations of all 4^{11} Pauli rotations. The overhead of this synthesis method is presented in Figure 13a). For Pauli-based computation [BSS16, Lit19, CC22] where universal quantum computation is implemented via magic state preparation and multi-qubit Pauli measurements, implementation of arbitrary Pauli measurements may be more interesting than Pauli rotations. Figure 13b) shows the results of a similar search, where the 288 native logical measurements are conjugated by Pauli rotations until all measurements are found.

If we are implementing a sequence of gates using (39) then we require three measurements per gate. However, depending on the support of the multi-qubit measurement the final measurement of one rotation circuit can be used as the initialization of the next rotation circuit. This would allow us to implement rotations using two measurements per rotation. Depending on the particular sequence of rotations, somewhere between two or three measurements per rotation are required.

5 Future Work

Ancilla systems are particularly affordable when only one layer of additional qubits is necessary. We were able to find logical operators on the gross code where this is the case. Are there any other families of codes where this is possible? Our analytical techniques did not suffice to prove that a monolayer system suffices

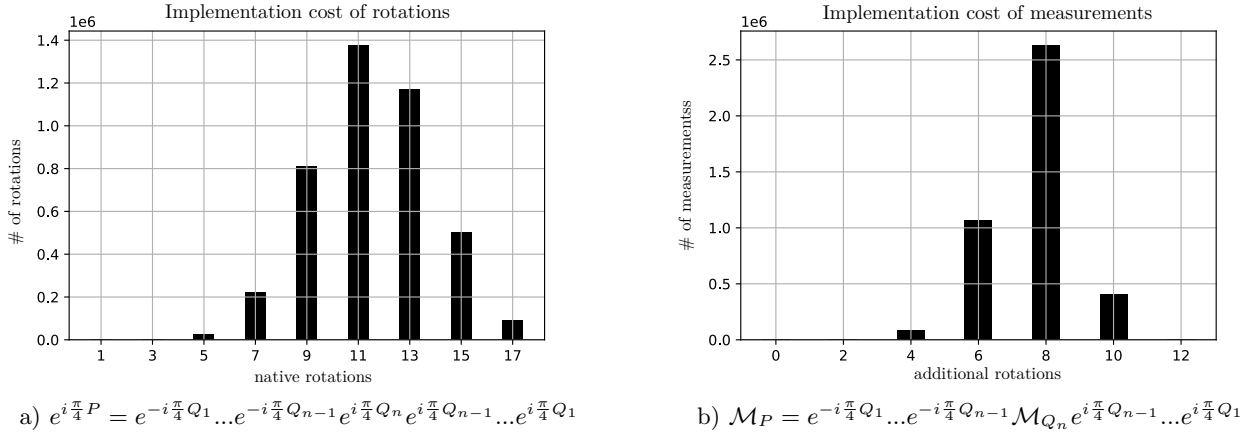


Figure 13: Partially optimized implementation costs of a) all 4^{11} Pauli rotations $e^{i\frac{\pi}{4}P}$ and b) all 4^{11} Pauli measurements \mathcal{M}_P . Cost is measured in the total number of rotation circuits (39) required to implement the gate using the form displayed beneath the figure.

for the gross code. Is it ever possible to prove that a single layer is enough? Quantum expander codes seem promising candidates.

Measurements using ancilla systems allow us to implement Clifford gates through techniques similar to lattice surgery [Lit19]. Can these methods be extended to inject physical magic states into a logical qubit? Such an operation could form the foundation for a magic state factory on an LDPC code.

We derived explicit syndrome circuits for the \bar{X} and \bar{Z} measurement schemes for the gross code. Are these syndrome circuits optimal in terms of the number of fault locations? Can one design optimal or otherwise high-performance syndrome circuits for other measurement schemes, perhaps assuming that the original code \mathcal{G} also has an efficient syndrome circuit?

From section 4.3 it is clear that implementing logical computations will require very many measurements, which in turn required several rounds of error correction. For certain error correction codes, such as perhaps [SHR24], is there a single-shot error correction scheme for merged codes?

Acknowledgements We are grateful to Ben Brown, John Blue, and Michael Beverland for enlightening discussions and valuable feedback.

A Appendices

A.1 Proofs for the X Ancilla System

In this appendix, we prove Theorem 1 for the X measurement scheme. We begin with an explicit description of the stabilizer check matrices H_L^X and H_L^Z , corresponding to the code \mathcal{G}_X . Recall that the matrices $J_{V_0} : \mathcal{V} \rightarrow V_0$ and $J_{C_0} : \mathcal{C}^Z \rightarrow C_0$ are projection isometries onto the subsets $V_0 \subset \mathcal{V}$ and $C_0 \subset \mathcal{C}^Z$ respectively. These define $F := J_{C_0}^\top H^Z J_{V_0}$ and the full-rank G satisfying $GF = 0$. We may also consider isometries $J_{V_i} : \mathcal{V} \cup V_1 \cup \dots \cup V_{i-1} \rightarrow V_i$ for all odd i that take elements in $V_0 \subset \mathcal{V}$ to their corresponding element in V_i , and similarly for $J_{C_i} : \mathcal{C}^Z \cup C_1 \cup C_2 \cup \dots \cup C_{i-1} \rightarrow C_i$. These give a convenient way of writing H_L^X and H_L^Z .

Having outlined the construction of \mathcal{G}_X , we show that it gives a valid code that features \bar{X}_M as a stabilizer, and has exactly one fewer qubit than \mathcal{G} .

Theorem 1. *Say \mathcal{G} is any CSS code and \bar{X}_M is a X -logical Pauli operator with no smaller X -logical operators in its support. Let \mathcal{G}_X be the code defined above. Then \bar{X}_M is a stabilizer of \mathcal{G}_X , and \mathcal{G}_X has exactly one fewer logical qubit than \mathcal{G} .*

Proof of Theorem 1. First we show that the checks defined by the matrices H_L^X and H_L^Z commute, which is equivalent to $H_L^X(H_L^Z)^\top = 0$. We follow their recursive definition. For the base case, since H^X and H^Z commute, we may restrict our attention to the qubits V_0, C_1 , and must show that the X checks on $V_1 : [I \ F^\top]$ commutes with the Z checks on $C_0 : [F \ I]$ and, if $L = 1$, $U_1 : [0 \ G]$.

$$X(V_1) \sim Z(C_0) : [I \ F^\top] \cdot [F \ I]^\top = F^\top + F^\top = 0, \quad (41)$$

$$X(V_1) \sim Z(U_1) : [I \ F^\top] \cdot [0 \ G]^\top = F^\top G^\top = 0, \quad (42)$$

since $GF = 0$ by definition of G . For the recursive case, we restrict our attention to qubits C_{L-2}, V_{L-1}, V_L . The X checks $V_{L-2} : [F^\top \ I \ 0]$ and $V_L : [0 \ I \ F^\top]$ should commute with the Z checks $C_{L-1} : [I \ F \ I]$. If this is the final layer, then we also need to include Z checks U_L . Note that X checks V_{L-2} and Z checks U_L commute since they act on disjoint sets of qubits.

$$X(V_{L-2}) \sim Z(C_{L-1}) : [F^\top \ I \ 0] \cdot [I \ F \ I]^\top = F^\top + F^\top = 0, \quad (43)$$

$$X(V_L) \sim Z(C_{L-1}) : [0 \ I \ F^\top] \cdot [I \ F \ I]^\top = F^\top + F^\top = 0, \quad (44)$$

$$X(V_L) \sim Z(U_L) : [0 \ I \ F^\top] \cdot [0 \ 0 \ G]^\top = F^\top G^\top = 0. \quad (45)$$

Second, we demonstrate that \bar{X}_M is a stabilizer in \mathcal{G}_X : it is simply the product of all the X stabilizers on all the V_i with odd i . To see this, we note that for odd $j < L$,

$$H_X(V_j) = X(V_{i-1})X(V_{i+1}). \quad (46)$$

The product is not supported on any of the C_j since all the individual contributions from each of the checks in V_j cancel. This is equivalent to the claim that each Z check on C_0 is supported on an even number of qubits in V_0 , which is guaranteed since \bar{X}_M , whose support is exactly V_0 , is a logical operator. Similarly, L is odd and $H_X(V_L) = X(V_{L-1})$, i.e. the product of checks in the final layer acts on all qubits in V_{L-1} . Therefore, we see that

$$\prod_{\substack{j=1 \\ j \text{ odd}}}^L X(V_j) = X(V_0) = \bar{X}_M. \quad (47)$$

Finally, we show that if \mathcal{G} has k logical qubits, then \mathcal{G}_X has $k-1$ logical qubits. We proceed by induction on the number of layers, and we use \mathcal{G}_X^l to indicate the merged code for measuring \bar{X}_M with l layers, and H_l^X, H_l^Z its parity check matrices.

Make the following observation: the checks U_L can be connected to any C_i for odd i , and hence we may as well assume they are always connected to C_1 . To see this, let (I, F, I) describe the Z checks in C_{2i} with the three components of the vector indicating the support on C_{2i-1}, V_{2i} , and C_{2i+1} , respectively. Then, suppose the checks U_L can be supported on C_{2i+1} (this is the case for $2i+1 = L$), so that $(0, 0, vG)$ represents some combination of these checks. We can move the checks to be entirely supported on C_{2i-1} by adding a combination of checks from C_{2i} , namely

$$(0, 0, vG) + vG(I, F, I) = (vG, 0, 0). \quad (48)$$

In other words, the gauge operators U_L have equivalent representatives over all C_i for odd i .

We begin the inductive proof starting with $L = 1$. If \mathcal{G} has n physical qubits, then we have $k = n - \text{rank}(H^X) - \text{rank}(H^Z)$. Then \mathcal{G}_X^1 has $n + |C_0|$ physical qubits. The rows of $\text{rank}(H_1^X)$ corresponding to V_1 form a linearly independent set (owing to their support on V_0), and no product of them can be in H^X . Therefore $\text{rank}(H_1^X) = \text{rank}(H^X) + |V_1|$.

Now we compute the rank of H_1^Z . We consider the null space $\text{null}(H_1^Z) = \{c \text{ s.t. } cH_1^Z = 0\}$, and show that it has the same dimension as $\text{null}(H^Z)$. Suppose $u \in U_1$ and $v \in \mathcal{C}_Z$ are Z checks such that their product is trivial. Then:

$$0 = [u \ v] H_1^Z = [u \ v] \begin{bmatrix} 0 & G \\ H^Z & J_{C_1} \end{bmatrix} = u [0 \ G] + v [H^Z \ J_{C_1}] \quad (49)$$

implying $vH^Z = 0$, so $|\text{null}(H_1^Z)| \leq |\text{null}(H^Z)|$. Conversely, suppose that $v \in \text{null}(H^Z)$. We claim there exists a vector u such that together u, v are in $\text{null}(H_1^Z)$. By the calculation above, this demands that $uG = vJ_{C_1}$, where we can view vJ_{C_1} as a Z Pauli product on C_1 . This Pauli operator is in the stabilizer by construction, and must hence commute with the X stabilizers supported on V_1 . The corresponding submatrix of H_1^X is $[J_{V_1} \ F^\top]$, so commutativity is equivalent to $F^\top(vJ_{C_1})^\top = 0$, so $(vJ_{C_1})F = 0$. Because the rows of G span $\text{null}(F)$, there must exist a u such that $uG = vJ_{C_1}$. We conclude that $|\text{null}(H_1^Z)| = |\text{null}(H^Z)|$. Hence:

$$\text{rank}(H_1^Z) = (m_z + |U_1|) - \dim(\text{null}(H^Z)) = \text{rank}(H^Z) + |U_1|. \quad (50)$$

The size of U_1 is the rank of G . Observe that the rank of F is $|V| - 1$, since we assumed that the only logical operator supported on V is \bar{X}_M . Therefore $|U_1| = \text{rank}(G) = |C_0| - \text{rank}(F) = |C_0| - |V_0| + 1$, and the number logical qubits in \mathcal{G}_X^1 is

$$n + |C_0| - \text{rank}(H_1^X) - \text{rank}(H_1^Z) = n - |V_0| + |C_0| - \text{rank}(H^X) - (\text{rank}(H^Z) + |U_1|) \quad (51)$$

$$= k - |V_0| + |C_0| - |U_1| \quad (52)$$

$$= k - |V_0| + |C_0| - (|C_0| - |V_0| + 1) = k - 1. \quad (53)$$

We proceed with the inductive step: assuming that \mathcal{G}_X^{L-2} has $k - 1$ logical qubits, we show the same for \mathcal{G}_X^L . The newly added set of X checks V_L is linearly independent. A product of any subset of V_L will have non-trivial support on C_L , and while $H_X(V_L) = X(V_{L-1})$ has no support on C_L , by assumption it cannot be a stabilizer in H_{L-2}^X . Similarly, the newly added Z checks C_{L-1} is linearly independent, and their products always have support on C_L . We conclude that \mathcal{G}_X^L has $k - 1$ logical qubits.

In fact, these $k - 1$ qubits are the remaining logical qubits from \mathcal{G} . For any \bar{Z} that commutes with \bar{X}_M , its support on V_0 is even in size, and as a consequence of Lemma 8, we can clean its support from V_0 by multiplying by Z checks of \mathcal{G} . This implies some $\bar{Z}' \equiv_{\mathcal{G}} \bar{Z}$ supported only on R , which is then also a logical operator of \mathcal{G}_X . For a logical operator $\bar{X} \not\equiv_{\mathcal{G}} \bar{X}_M$ of \mathcal{G} supported only on $V_0 \cup R$, notice that \bar{X} is also a logical operator of \mathcal{G}_X . It is nontrivial in \mathcal{G}_X because there was some \bar{Z} that anticommuted with \bar{X} in \mathcal{G} and commuted with \bar{X}_M , and therefore the construction of \bar{Z}' still anticommutes with \bar{X} in \mathcal{G}_X . \square

A.2 Proofs for the Y Ancilla System

Theorem 18. *The Y -system encodes $k - 1$ qubits.*

Proof. We omit the proof of commutativity, since all checks commute as they do in the X and Z measurement ancilla patches, respectively. Similarly, it is straightforward to see that the operator $\bar{X}_M \bar{Z}_M$ is a product of stabilizers in the final code, as we can take the product of all checks in the interface and two modules. We prove the number of logical qubits by an induction argument on the rank of the symplectic parity check matrix \mathcal{H} . This matrix describes parity checks as row vectors of length $2n$, where the first n bits specify the locations of Pauli X and the last n specify the locations of Pauli Z , which is standard for non-CSS codes. One can write \mathcal{H} down explicitly using Figure 7.

We first note that Lemma 16 implies that there are as many linearly independent checks in U^B as there are qubits in B . Therefore, the addition of U^B and B does not change the logical qubit count, so next we analyze the Y -system without them. This eliminates $|B|$ rows and $|B|$ columns from \mathcal{H} .

To begin the induction, consider the case $L = 1$, where we have $n + |C^X| + |C^Z|$ many physical qubits. We compute the dimension of the row nullspace of \mathcal{H} , $\text{null}(\mathcal{H})$. Suppose there is a set of checks whose product acts trivially on all qubits. First, observe that the check corresponding to q_1 cannot be in this set. This is because the check on q_1 acts as Y on the qubit q_0 , which means for the product of checks to act as identity on q_0 , we need a collection of X -checks on \mathcal{G} that multiply to identity on all of \mathcal{G} except W_0^Y , and similarly a collection of Z -checks from \mathcal{G} that multiply to identity on all of \mathcal{G} except q_0 . Such collections cannot exist as their product will anti-commute. Let \mathcal{H}' be the matrix \mathcal{H} with the row q_1 removed, we see that $\text{null}(\mathcal{H}) = \text{null}(\mathcal{H}')$.

With all the non-CSS check removed, we can now bound $\dim(\text{null}(\mathcal{H}'))$ by computing the redundancies in X -checks and Z -checks separately. Using the same argument as in the proof of Theorem 1, we have

$$\dim(\text{null}(\mathcal{H})) = \dim(\text{null}(\mathcal{H}')) = \dim(\text{null}(H^X)) + \dim(\text{null}(H^Z)).$$

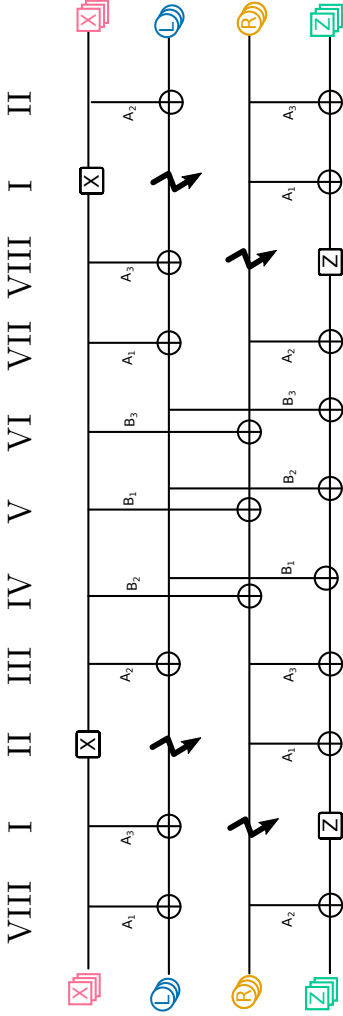
Therefore,

$$\begin{aligned} \text{rank}(\mathcal{H}) &= m_X + m_Z + |V^X| + |V^Z| - 1 + |U^X| + |U^Z| - \dim(\text{null}(H^X)) - \dim(\text{null}(H^Z)) \\ &= \text{rank}(H^X) + \text{rank}(H^Z) + |C^X| + |C^Z| + 1, \end{aligned}$$

which implies the number of logical qubits is $k - 1$.

Inductively, we make the same observation as in the proof of Theorem 1: the newly added set of X checks V_L^X is linearly independent. Any $H_X(v \in V_L^X)$ will have non-trivial support on C_L , and while $H_X(V_L^X) = X(V_{L-1})$ has no support on C_L , by assumption it cannot be a stabilizer in \mathcal{G}_Y^{L-2} . Similarly, the newly added Z checks in C_{L-1}^X are linearly independent, and their products always have support on C_L . We conclude that \mathcal{G}_Y^L has $k - 1$ logical qubits, which are the original logical qubits from \mathcal{G} . \square

a) Gross Code Syndrome Circuit



b) X System Merged Syndrome Circuit

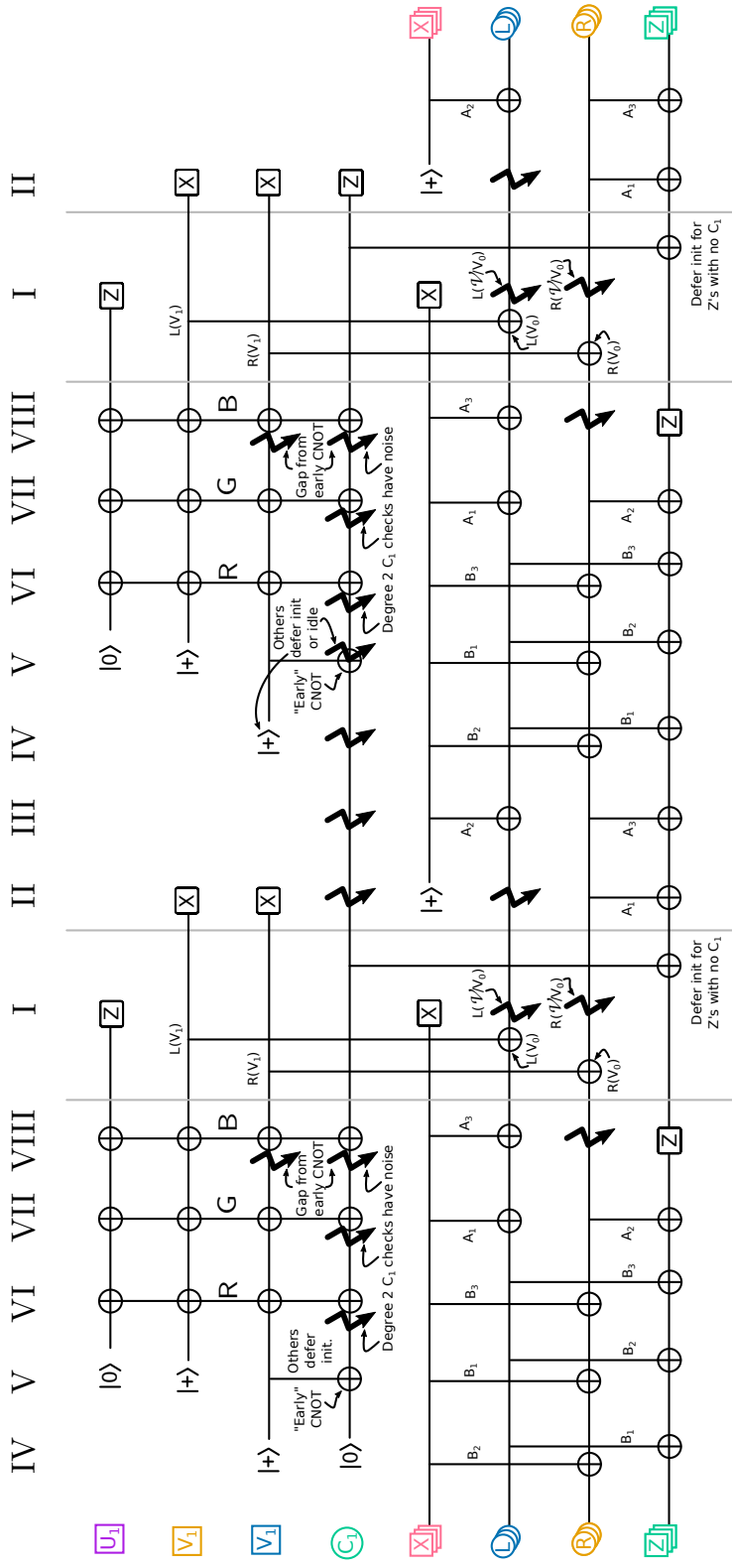
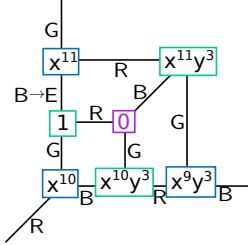
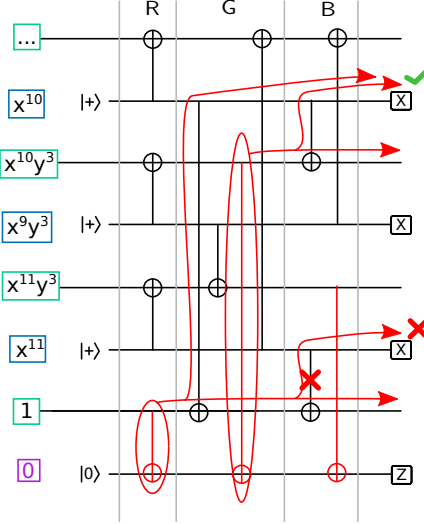


Figure 14: Syndrome circuits used for the numerical experiments. a) The original syndrome circuit for the gross code from [BCG⁺24]. b) Two cycles of the merged syndrome circuit for an X ancilla system. The gates marked R, G, B denote single layers of CNOTs determined by an edge-coloring of Figure 10, corrected by the procedure in Figure 15. Lightning bolts denote idle errors.

a) Subgraph of Graph Coloring



b) Original Coloring Circuit with Incorrect Syndromes



c) Corrected Circuit via Early CNOTs

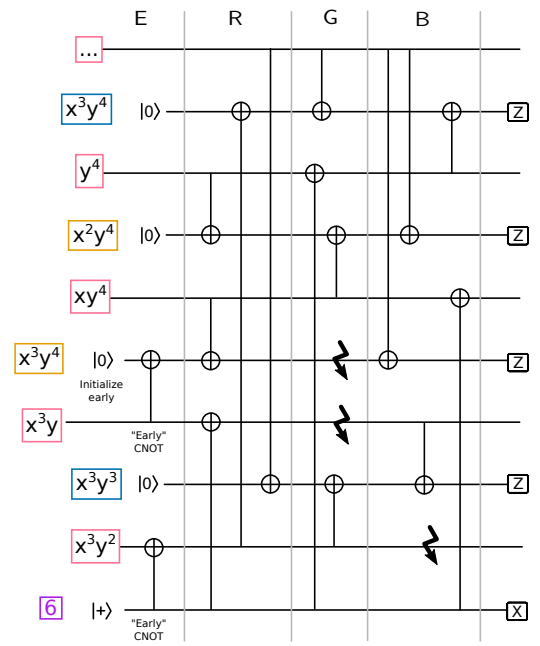
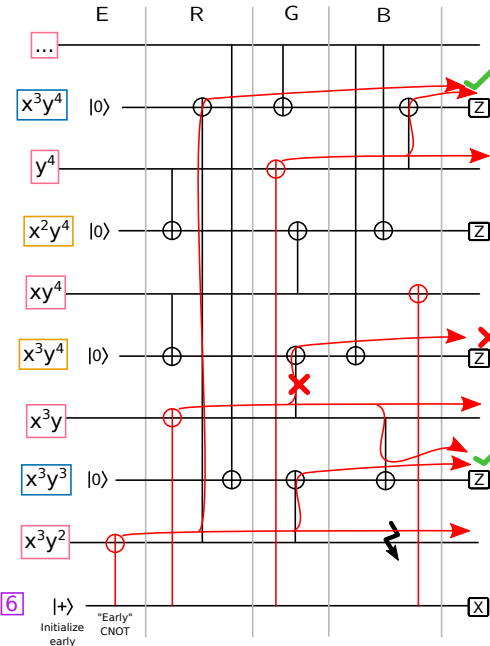
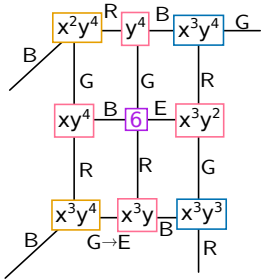
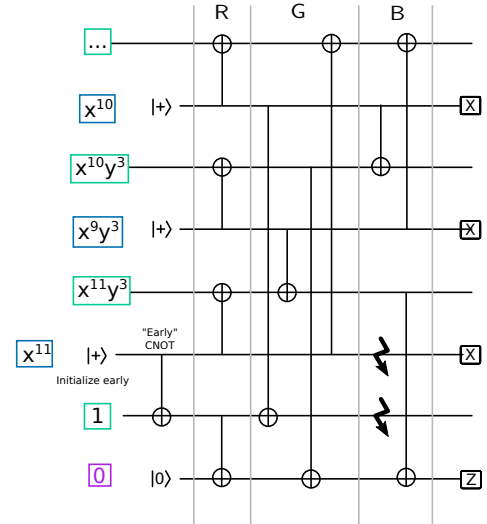


Figure 15: Procedure for correcting the syndrome circuit of the X and Z ancilla systems (top and bottom respectively) from the edge-coloring. a) Subregion of the Tanner graph in Figure 10 with a mixture of X and Z checks, hence resulting in incorrectly computed syndromes. b) Incorrect circuit with the support of the gauge stabilizer propagated to the end of the circuit. We see that this stabilizer is now supported on some of the *check* qubits, which is wrong. We see that there is a particular CNOT gate that is responsible. c) Corrected circuit where the responsible CNOT is moved to the front. Lightning bolts denote idle errors.

References

[ABO08] D. Aharonov and M. Ben-Or. Fault-tolerant quantum computation with constant error. *SIAM J. Sci. Comput.*, 38:176–188, 2008.

[AGP05] P. Aliferis, D. Gottesman, and J. Preskill. Quantum accuracy threshold for concatenated distance-3 codes. *arXiv:quant-ph/0504218v3*, 2005.

[AI23] Google Quantum AI. Suppressing quantum errors by scaling a surface code logical qubit. *Nature*, 614:676–681, 2023.

[BB24] N. P. Breuckmann and S. Burton. Fold-transversal clifford gates for quantum codes, 2024.

[BCG⁺24] S. Bravyi, A. W. Cross, J. M. Gambetta, D. Maslov, P. Rall, and T. J. Yoder. High-threshold and low-overhead fault-tolerant quantum memory. *Nature*, 627(8005):778–782, March 2024.

[BDS⁺24] N. Berthelsen, D. Devulapalli, E. Schoute, A. M. Childs, M. J. Gullans, A. V. Gorshkov, and D. Gottesman. Toward a 2d local implementation of quantum ldpc codes. *arXiv:2404.17676*, 2024.

[BE21a] N. P. Breuckmann and J. N. Eberhardt. Balanced product quantum codes. *IEEE Transactions on Information Theory*, 67(10):6653–6674, 2021.

[BE21b] N. P. Breuckmann and J. N. Eberhardt. Quantum low-density parity-check codes. *PRX Quantum*, 2(040101), 2021.

[BHK24] M. E. Beverland, S. Huang, and V. Kliuchnikov. Fault tolerance of stabilizer channels. *arXiv preprint arXiv:2401.12017*, 2024.

[BK98] S. Bravyi and A. Yu. Kitaev. Quantum codes on a lattice with boundary. *arXiv:quant-ph/9811052*, 1998.

[BK05] S. Bravyi and A. Kitaev. Universal quantum computation with ideal clifford gates and noisy ancillas. *Phys. Rev. A*, 71(022316), 2005.

[BMT⁺22] M. E. Beverland, P. Murali, M. Troyer, K. M. Svore, T. Hoefler, V. Kliuchnikov, G. H. Low, M. Soeken, A. Sundaram, and A. Vaschillo. Assessing requirements to scale to practical quantum advantage. *arXiv:2211.07629*, 2022.

[BPT10] S. Bravyi, D. Poulin, and B. Terhal. Tradeoffs for reliable quantum information storage in 2d systems. *Phys. Rev. Lett.*, 104(050503), 2010.

[BSS16] S. Bravyi, G. Smith, and J. A. Smolin. Trading classical and quantum computational resources. *Physical Review X*, 6(2), June 2016.

[BVC⁺17] N. P. Breuckmann, C. Vuillot, E. Campbell, A. Krishna, and B. M. Terhal. Hyperbolic and semi-hyperbolic surface codes for quantum storage. *Quantum Sci. Technol.*, 2(035007), 2017.

[Cal76] D. Callan. The generation of $sp(f2)$ by transvections. *Journal of Algebra*, 42:378–390, 1976.

[CC22] C. Chamberland and E. T. Campbell. Universal quantum computing with twist-free and temporally encoded lattice surgery. *PRX Quantum*, 3(1), February 2022.

[CKBB22] L. Z. Cohen, I. H. Kim, S. D. Bartlett, and B. J. Brown. Low-overhead fault-tolerant quantum computing using long-range connectivity. *Science Advances*, 8(20):eabn1717, 2022.

[Cow24] A. Cowtan. Ssip: automated surgery with quantum ldpc codes. *arXiv:2407.09423*, 2024.

[CTV17] E. T. Campbell, B. M. Terhal, and C. Vuillot. Roads towards fault-tolerant universal quantum computation. *Nature*, 549:172–179, 2017.

[DA07] D. P. DiVincenzo and P. Aliferis. Effective fault-tolerant quantum computation with slow measurements. *Physical Review Letters*, 98(2), January 2007.

[DKLP02] E. Dennis, A. Kitaev, A. Landahl, and J. Preskill. Topological quantum memory. *J. Math. Phys.*, 43:4452–4505, 2002.

[ES24] J. N. Eberhardt and V. Steffan. Logical operators and fold-transversal gates of bivariate bicycle codes. *arXiv:2407.03973v1*, 2024.

[FGL20] O. Fawzi, A. Gospellier, and A. Leverrier. Constant overhead quantum fault tolerance with quantum expander codes. *Communications of the ACM*, 64(1):106–114, 2020.

[FMMC12] A. G. Fowler, M. Mariantoni, J. M. Martinis, and A. N. Cleland. Surface codes: Towards practical large-scale quantum computation. *Phys. Rev. A*, 86(032324), 2012.

[GC99] D. Gottesman and I. Chuang. Demonstrating the viability of universal quantum computation using teleportation and single-qubit operations. *Nature*, 402:390–393, 1999.

[GCR24] A. Gong, S. Cammerer, and J. M. Renes. Toward low-latency iterative decoding of qldpc codes under circuit-level noise. *arXiv:2403.18901*, 2024.

[GE21] C. Gidney and M. Ekera. How to factor 2048 bit rsa integers in 8 hours using 20 million noisy qubits. *Quantum*, 5(433), 2021.

[Gid21] C. Gidney. Stim: a fast stabilizer circuit simulator. *Quantum*, 5:497, July 2021.

[Got97] D. Gottesman. Stabilizer codes and quantum error correction. *arXiv:quant-ph/9705052*, 1997.

[Got09] D. Gottesman. An introduction to quantum error correction and fault-tolerant quantum computation. *arXiv:0904.2557v1*, 2009.

[Got14] D. Gottesman. Fault-tolerant quantum computation with constant overhead. *Quantum Information & Computation*, 14:1338–1372, 2014.

[Has21] M. B. Hastings. On quantum weight reduction. *arXiv:2102.10030*, 2021.

[HB23] O. Higgott and N. P. Breuckmann. Constructions and performance of hyperbolic and semi-hyperbolic floquet codes. *arXiv:2308.03750*, 2023.

[HFDM12] D. Horsman, A. G. Fowler, S. Devitt, and R. Van Meter. Surface code quantum computing by lattice surgery. *New J. Phys.*, 14(123011), 2012.

[HG23] O. Higgott and C. Gidney. Sparse blossom: correcting a million errors per core second with minimum-weight matching. *arXiv preprint arXiv:2303.15933*, 2023.

[HJOY23] S. Huang, T. Jochym-O’Connor, and T. J. Yoder. Homomorphic logical measurements. *PRX Quantum*, 4(030301), 2023.

[JO19] T. Jochym-O’Connor. Fault-tolerant gates via homological product codes. *Quantum*, 3(120), 2019.

[Kit97] A. Yu. Kitaev. *Quantum Error Correction with Imperfect Gates*, pages 181–188. Springer US, 1997.

[KLR⁺22] S. Krinner, N. Lacroix, A. Remm, A. Di Paolo, E. Genois, C. Leroux, C. Hellings, S. Lazar, F. Swiadek, J. Herrmann, G. J. Norris, C. K. Andersen, M. Muller, A. Blais, C. Eichler, and A. Wallraff. Realizing repeated quantum error correction in a distance-three surface code. *Nature*, 605:669–674, 2022.

[KLZ98] E. Knill, R. Laflamme, and W. Zurek. Resilient quantum computation. *Science*, 279:342–345, 1998.

[Kni05] E. Knill. Scalable quantum computing in the presence of large detected-error rates. *Phys. Rev. A*, 71(042322), 2005.

[KP21] A. Krishna and D. Poulin. Fault-tolerant gates on hypergraph product codes. *Phys. Rev. X*, 11(011023), 2021.

[LB18] A. Lavasani and M. Barkeshli. Low overhead clifford gates from joint measurements in surface, color, and hyperbolic codes. *Phys. Rev. A*, 98(052319), 2018.

[Li15] Y. Li. A magic state’s fidelity can be superior to the operations that created it. *New J. Phys.*, 17(023037), 2015.

[Lit19] D. Litinski. A game of surface codes: Large-scale quantum computing with lattice surgery. *Quantum*, 3:128, March 2019.

[LZ22] A. Leverrier and G. Zemor. Quantum tanner codes. *arXiv:2202.13641*, 2022.

[NFB17] H. Poulsen Nautrup, N. Friis, and H. J. Briegel. Fault-tolerant interface between quantum memories and quantum processors. *Nature communications*, 8(1):1321, 2017.

[PGP⁺24] C. Poole, T. M. Graham, M. A. Perlin, M. Otten, and M. Saffman. Architecture for fast implementation of qldpc codes with optimized rydberg gates. *arXiv:2404.18809*, 2024.

[PK21] P. Panteleev and G. Kalachev. Degenerate quantum ldpc codes with good finite length performance. *Quantum*, 5(585), 2021.

[PK22] P. Panteleev and G. Kalachev. Asymptotically good quantum and locally testable classical ldpc codes. In *Proceedings of the 54th Annual ACM SIGACT Symposium on Theory of Computing*, STOC 2022, pages 375–388, New York, NY, USA, 2022. Association for Computing Machinery.

[QWV23] A. O. Quintavalle, P. Webster, and M. Vasmer. Partitioning qubits in hypergraph product codes to implement logical gates. *Quantum*, 7(1153), 2023.

[Rof22] J. Roffe. LDPC: Python tools for low density parity check codes, 2022.

[RWBC20] J. Roffe, D. R. White, S. Burton, and E. Campbell. Decoding across the quantum low-density parity-check code landscape. *Physical Review Research*, 2(4), Dec 2020.

[SGI⁺24] E. Sabo, L. G. Gunderman, B. Ide, M. Vasmer, and G. Dauphinais. Weight reduced stabilizer codes with lower overhead. *arXiv:2402.05228*, 2024.

[SHR24] T. R. Scruby, T. Hillmann, and J. Roffe. High-threshold, low-overhead and single-shot decodable fault-tolerant quantum memory. *arXiv:2406.14445*, 2024.

[SI05] A. M. Steane and B. Ibinson. Fault-tolerant logical gate networks for calderbank-shor-steane codes. *Phys. Rev. A*, 72(052335), 2005.

[SYK⁺23] N. Sundaresan, T. J. Yoder, Y. Kim, M. Li, E. H. Chen, G. Harper, T. Thorbeck, A. W. Cross, A. D. Corcoles, and M. Takita. Demonstrating multi-round subsystem quantum error correction using matching and maximum likelihood decoders. *Nature Communications*, 14(2852), 2023.

[TZ14] J.-P. Tillich and G. Zemor. Quantum ldpc codes with positive rate and minimum distance proportional to the square root of the blocklength. *IEEE Transactions on Information Theory*, 60(1193), 2014.

[VLC⁺19] C. Vuillot, L. Lao, B. Criger, C. G. Almudever, K. Bertels, and B. Terhal. Code deformation and lattice surgery are gauge fixing. *New Journal of Physics*, 21(033028), 2019.

[VXHB24] L. Voss, S. J. Xian, T. Haug, and K. Bharti. Trivariate bicycle codes. *arXiv:2406.19151*, 2024.

[VYL⁺23] J. Viszlai, W. Yang, S. F. Lin, J. Liu, N. Nottingham, J. M. Baker, and F. T. Chong. Matching generalized-bicycle codes to neutral atoms for low-overhead fault-tolerance. *arXiv:2311.16980*, 2023.

[WB24] S. Wolanski and B. Barber. Ambiguity clustering: an accurate and efficient decoder for qldpc codes. *arXiv:2406.14527*, 2024.

[XAP⁺24] Q. Xu, J. P. Bonilla Ataides, C. A. Pattison, N. Raveendran, D. Bluvstein, J. Wurtz, B. Vasić, M. D. Lukin, L. Jiang, and H. Zhou. Constant-overhead fault-tolerant quantum computation with reconfigurable atom arrays. *Nature Physics*, pages 1–7, 2024.

[ZSP⁺23] G. Zhu, S. Sikander, E. Portnoy, A. W. Cross, and B. J. Brown. Non-clifford and parallelizable fault-tolerant logical gates on constant and almost-constant rate homological quantum ldpc codes via higher symmetries. *arXiv:2310.16982*, 2023.